

Journal type: Original Article

**Integrative taxonomy of insular land snails of the genus *Sicradiscus* Páll-Gergely, 2013
(Gastropoda, Plectopylidae) with description of a new species**

urn:lsid:zoobank.org:pub:814EED13-7D1A-4215-BCCF-2A36FA3797C8

Running title: **Integrative taxonomy of insular *Sicradiscus***

Naoto Sawada¹ | Chung-Chi Hwang² | Josef Harl³ | Takafumi Nakano¹

¹Department of Zoology, Graduate School of Science, Kyoto University, Kyoto, Japan

²Department of Life Sciences, National University of Kaohsiung, Kaohsiung, Taiwan

³Institute of Pathology, University of Veterinary Medicine, Vienna, Vienna, Austria

Correspondence

Naoto Sawada, Department of Zoology, Graduate School of Science, Kyoto University,
Kyoto, Japan

Email: sawada.naoto.82w@st.kyoto-u.ac.jp

KEYWORDS

canonical variates analysis, Iriomote Island, molecular phylogeny, Ryukyu Islands,
Sicradiscus pallgergelyi sp. nov.

Funding information

- 26 Japan Society for the Promotion of Science, Grant/Award Number: JP21J22917; the Tokyo
27 Metropolitan University Fund for TMU Strategic Research, Grant/Award Number: FY2020–
28 FY2022.

Abstract

Many land snail taxa have undergone speciation in the Ryukyu Islands and Taiwan in East Asia. We examined the shell, radular, and genital morphology, and mitochondrial phylogeny of two described *Sicradiscus* species distributed in Miyako Island and Taiwan, and the newly discovered *S. pallgergelyi* sp. nov. from Iriomote Island. Canonical variates analysis based on adult shell measurements indicated that *S. pallgergelyi* sp. nov. and the Taiwanese *S. ishizakii* had more similar shell measurements, whereas *S. pallgergelyi* sp. nov. shared common characteristics of shell sculpture with the Japanese *S. hirasei*. The leave-one-out cross-validation results correctly classified 100%, 71.4%, and 88.0% of *S. hirasei*, *S. ishizakii*, and *S. pallgergelyi* sp. nov., respectively. The radular and genital morphology was similar in these three species. Moreover, molecular phylogenetic analyses showed monophyly of the three species, although the Japanese lineages were more closely related to each other than to the Taiwanese species. Accordingly, the characteristics of shell sculpture are common traits of the two Japanese species, and these findings indicate that shell morphology has significantly diverged in Japan. The different apertural callus lengths among the three species may be an adaptation to predators, and shell flatness may reflect interspecific differences in microhabitats.

1 | INTRODUCTION

The land snail family Plectopylidae consists of 113 extant species and seven fossil species which are distributed in Asia from the southern Himalayan region (Nepal) to the Ryukyu Islands and the Malay Peninsula, and their distribution includes northeastern India, Myanmar, Thailand, Laos, Vietnam, China, and Taiwan (MolluscaBase eds, 2021; Páll-Gergely, 2018b; Páll-Gergely, Budha, Naggs, Backeljau, & Asami, 2015a; Páll-Gergely & Hunyadi, 2013). Plectopylidae are characterized by having depressed shells with internal plicae and lamellae that are approximately a quarter to a half whorl behind the aperture. Before Páll-Gergely and Hunyadi (2013), the extant members of the family had been classified into four genera, which were originally established as “sections” under the genus *Plectopylis* Benson, 1860 by Gude (1899). Although the traditional classification was only based on a few shell characters, recent comprehensive examinations of shells, radulae, and reproductive organs resulted in the description of five further extant genera (Páll-Gergely & Hunyadi, 2013; Páll-Gergely et al., 2015b; Páll-Gergely, Muratov, & Asami, 2016). Plectopylidae are currently divided into two subfamilies, Plectopylinae and Sinicolinae, mostly based on reproductive anatomical traits and the fine sculpture of the protoconch (Páll-Gergely, 2018b).

The range of the sinicoline genus *Sicradiscus* Páll-Gergely, 2013 extends from northern Vietnam and the Chinese provinces Sichuan and Yunnan to Miyako Island in the Ryukyu Islands, the easternmost distribution range of the family. Most *Sicradiscus* species are indigenous to the Asian continent. Only two species, *S. hirasei* (Pilsbry, 1904) and *S. ishizakii* (Kuroda, 1941), were described from Miyako Island in the Ryukyu Islands and Taiwan, respectively, which are the eastern margin of the distribution of the genus (Páll-Gergely & Hunyadi, 2013).

Sicradiscus has two species groups. Four species [*Sicradiscus feheri* Páll-Gergely & Hunyadi, 2013, *S. mansuyi* (Gude, 1908), *S. invius* (Heude, 1885), and *S. securus* (Heude, 1889)] inhabit Vietnam and the Chinese Sichuan, Yunnan, and Guangxi Provinces; these

species are characterized by the presence of an apertural fold and a rounded body whorl (herein, the “western group”). In contrast, the other species group includes five species [*S. cutisculptus* (Möllerndorff, 1882), *S. diptychia* (Möllerndorff, 1885), *S. hirasei*, *S. ishizakii*, *S. schistoptychia* (Möllerndorff, 1886)] that are distributed in the Chinese Hunan, Hubei, Fujian, and Zhejiang Provinces, in Taiwan, and in the Ryukyu Islands; these species are characterized by the absence of an apertural fold and a shouldered body whorl (herein, the “eastern group”) (Páll-Gergely & Hunyadi 2013). *Sicradiscus transitus* Páll-Gergely, 2013 from Guangxi and Guizhou Provinces forms a morphological connection between the two groups because the species possesses an apertural fold and a shouldered body whorl (Páll-Gergely & Hunyadi 2013).

Knowledge regarding the shell, radular, and genital morphology of insular species has been accumulated within the genus. Substantial variation was observed in plical and lamellar morphology of *S. hirasei* (Páll-Gergely, 2018a). In addition, morphological characters of reproductive organs of the two insular snails were revealed in the 1900s (Azuma & Azuma, 1984; Chang & Ookubo, 1999). Nevertheless, characterization of the reproductive anatomy of *S. hirasei* was amended in a subsequent publication (Páll-Gergely, 2018a), and that of *S. ishizakii* in Chang & Ookubo (1999) contains several descriptions which are difficult to interpret. Morphological characters of insular species have not been compared within genera in a series of detailed examinations (e.g. Páll-Gergely and Hunyadi 2013, Páll-Gergely et al., 2015b). Accordingly, accumulating information on morphological traits of this genus and conducting comprehensive comparisons can improve our understanding of insular and continental *Sicradiscus* species.

The first author recently discovered living *Sicradiscus* snails from Iriomote Island, which is located between Miyako Island and Taiwan. In this study, we performed integrative comparisons using adult shell, radular, and genital morphology, and mitochondrial COI sequences of *S. hirasei*, *S. ishizakii*, and the snails from Iriomote Island. As a result of our

examination, the information on the two described species has been updated. Furthermore, the detected interspecific morphological variation indicates the existence of different selection pressures on the snails in each island. Finally, the *Sicradiscus* snails from Iriomote Island were described as a new species, *S. pallgergelyi* sp. nov. by the first and last authors.

2 | MATERIALS AND METHODS

2.1 | Sample collection

In total, 64 *Sicradiscus* snails were newly collected. Twenty-five specimens of *S. pallgergelyi* sp. nov., 17 of *S. hirasei*, and 21 of *S. ishizakii* were examined morphologically; among these specimens, six individuals of *S. pallgergelyi* sp. nov., six of *S. hirasei* and three of *S. ishizakii* were used for the molecular phylogenetic analysis (Table 1). The field survey was conducted by the first and second authors from four localities in Japan and Taiwan, in 1997–2020 (Table 1; Figure 1). *Sicradiscus hirasei* was collected from crevices in the limestone on the ground in the inland natural forest of Miyako Island. On Iriomote Island, the new species was found in the inland natural forest at an elevation of around 200 m; however, *S. pallgergelyi* sp. nov. was not found from three limestone areas at low elevations whose environments are similar to the habitat of *S. hirasei* in Miyako Island. All of the snails collected by the first and second authors were found on the forest ground by eye. Because *S. hirasei* is protected by a Miyakojima City ordinance on Miyako Island, the snails were collected with permission by the city. In addition to the three insular species, a specimen of the continental *S. schistoptychia* (the type species of *Sicradiscus*) was included in the phylogenetic analysis.

Specimens from Iriomote and Miyako Islands were separated into shells and soft parts after being boiled in hot water at 80°C for 12 s. The extracted soft bodies were frozen until dissection after cutting off the foot tip. Separated tissues were preserved in 99% ethanol for molecular phylogenetic analysis. Snails from Taiwan were preserved in 95% ethanol after

boiling. The newly collected specimens in this study were deposited in the Zoological Collection of Kyoto University (KUZ).

2.2 | Morphological examination

Morphometric characters of the newly collected specimens and the type specimens of *S. hirasei* and *S. ishizakii* were examined. Fully matured adults were observed and measured following the methods in previous studies (Páll-Gergely et al., 2015b). The nomenclature of plicae and radulae follows Páll-Gergely & Hunyadi (2013) and Páll-Gergely (2018b), respectively. Newly collected specimens were first photographed using a Nikon D7100 camera with a Tamron SP 90 mm f/2.8 1:1 macro lens for Nikon. All specimen measurements were obtained from digital images of dorsal, ventral, and lateral sides of shells using ImageJ 1.51k (Schneider, Rasband, & Eliceiri, 2012). The apertural callus length was obtained from photos taken of the callus in the frontal position and was measured at the longest part of the callus. The spire angle was measured as the angle between the lines connecting shoulders of the apical and body whorls (Figure 2a). The umbilicus width was measured by extending the line connecting the base of the thickened aperture with the centre of the spiral (Figure 2b). The whorl number of adult shells was counted in intervals of 0.25 following the method described by Sawada & Nakano (2021). The numbers of specimens used for each character are shown in Table 2.

After obtaining measurements, microstructures of the protoconch and ventral side were observed in 10 adult shells of each species with a Hitachi TM1000 scanning electron microscope (SEM; Hitachi, Tokyo, Japan). The plical and lamellar morphology was studied in eight specimens of each species by carefully cracking open the shells. These inner structures of holotype of *S. pallgergelyi* sp. nov. were observed from the outside of the shell using transmitted light. Additionally, soft parts of three *S. ishizakii* specimens were extracted by breaking shells. Six *S. hirasei*, three *S. ishizakii*, and eight Iriomote Island specimens were

dissected under a Leica M125C stereoscopic microscope. The reproductive organ structure of the Japanese snails was photographed after fixation with 70% ethanol. Following the dissection of reproductive organs, the radulae were extracted by soaking oral tissues in 1 M sodium hydroxide solution for a day. Extracted radulae were coated with gold using a JFC-1200 Fine Coater (JEOL, Tokyo, Japan) and photographed with an SEM.

A canonical variates analysis (CVA) was conducted to clarify the relationships of shell measurements among the three *Sicradiscus* species. The CVA was performed on the datasets using five measurements, apertural callus length, shell diameter, shell height, and whorl number, and spire angle. Missing values of apertural callus length were substituted with the measurement average. The CVA data were also used to assign specimens with a leave-one-out cross-validation to estimate the expected actual error rates in classifying the insular *Sicradiscus* species. The CVA was conducted with PAST 4.04 (Hammer, Harper, & Ryan, 2001).

Abbreviations. Museum collections: ANSP, Academy of Natural Sciences, Philadelphia, USA; NCP, paratype collection of the Nishinomiya Shell Museum, Hyogo, Japan.

Morphometrics: BWL, body whorl length; CL, apertural callus length; D, shell diameter; EN, the number of embryos; H, shell height; HD, the proportion of H to D; SA, spire angle; UD, the proportion of umbilicus width to D; UW, umbilicus width; WN, whorl number. Radulae: EcL, ectocone of a lateral tooth; EcM, ectocone of a marginal tooth; EnL, endocone of a lateral tooth; EnM, endocone of a marginal tooth.

2.3 | PCR and DNA sequencing

The phylogenetic relationships of the insular *Sicradiscus* species and the continental *S. schistoptychia* were estimated using a mitochondrial marker, a fragment of the cytochrome *c* oxidase subunit I (COI) gene. Genomic DNA was extracted from muscle tissue of feet following the method described in Okamoto et al. (2006). A 706 bp section which

contains the COI region were amplified for 16 *Sicradiscus* snails by polymerase chain reaction (PCR) using a Takara Ex Taq kit (Takara Bio, Kusatsu, Japan) and the primers shown in Table 3 with a GeneAmp PCR System 9700 (Thermo Fisher Scientific, Waltham, MA, USA). The thermocycling regime was an initial denaturation step at 96°C for 1 min, followed by 35 cycles of 1 min at 96°C, 30 s at 42°C, and 1 min at 72°C, and a final extension at 72°C for 7 min. The PCR products were purified as described by Okamoto and Hikida (2009).

Nucleotide sequencing was conducted for PCR products using a BigDye Terminator v3.1 Cycle Sequencing Kit (Thermo Fisher Scientific, Waltham, MA, USA). The sequencing mixtures were heated to 96°C for 1 min, followed by 25 cycles at 96°C (10 s each), 45°C (30 s each), and 60°C (4 min each). Sequencing was then performed using an Applied Biosystems 3130xl Genetic Analyzer (Thermo Fisher Scientific, Waltham, MA, USA). The final alignment for the phylogenetic tree reconstructions included 16 sequences which had a length of 655 sites (see Alignment S1). The sequences were deposited in the International Nucleotide Sequence Database Collaboration through the DNA Databank of Japan (LC638856–LC638871).

2.4 | Molecular phylogenetic analyses

Phylogenetic trees were reconstructed using maximum likelihood (ML) with IQ-TREE v. 1.6.12 (Nguyen, Schmidt, von Haeseler, & Minh, 2015). The following best-fit models for each partition of the COI sequence were identified based on the corrected Akaike information criterion and the greedy algorithm: HKY+F for the 1st position, K2P for the 2nd position, and F81+F for the 3rd position. The robustness of the ML phylogenetic tree was inferred by 1000 non-parametric bootstrap replicates. Genetic distances among the three insular *Sicradiscus* species were estimated with the Kimura two-parameter (K2P) in MEGA v. 10.2.4 (Stecher, Tamura, & Kumar, 2020).

3 | RESULTS

3.1 | Morphological analyses

The morphometric character measurements are described in Table 2. The EN, H, UD, and WN measurements largely overlapped among the three *Sicradiscus* species. Although *S. ishizakii* shared similar BWL, D, HD, and UW measurements with *S. pallgergelyi* sp. nov., these characters distinguished *S. hirasei* from the two former species. The characters of CL and SA separated the three species with a slight overlap.

The first and second canonical components explained 90.5% and 100% of the total variance, respectively (Table 4). The variance of CV1 was mainly explained by SA and D. The two canonical components clearly distinguished *S. hirasei* from the other two congeners. The CVA results also showed that the shell morphology of *S. pallgergelyi* sp. nov. partly overlapped with that of *S. ishizakii* (Figure 3). The results of the leave-one-out cross-validation correctly classified 100%, 71.4%, and 88.0% of *S. hirasei*, *S. ishizakii*, and *S. pallgergelyi* sp. nov., respectively.

The upper whorl surface of the protoconch was smooth or very finely ribbed in *S. hirasei* and the new species, whereas *S. ishizakii* usually possessed remarkable ribs across its entire protoconch surface (Figure 4a,e,i). *Sicradiscus ishizakii* was also clearly distinguishable from its two congeners by the microstructure of the shell's ventral side (Figure 4b,f,j). *Sicradiscus ishizakii* had a glossed ventral side with rudimental radial striations, whereas the two other species had strong spiral striations reticulated with radial sculptures.

The lamellae shapes were approximately similar in the two Japanese species, although their morphology showed large variation (Figures 4c,g,k, 5a,c,e,g,i,k,m,o,q,s,u,w,y,aa,ac,ae,ag,ai,ak,am,ao,aq,as,au). The anterior lamellae of *S. hirasei* and *S. pallgergelyi* sp. nov. were narrow and elongated, and T-shaped (Figure 4c,k).

Alternatively, *S. ishizakii* had thick C-shaped anterior lamellae (Figure 4g). Among the three species, no significant differences were detected in the plicae (Figures 4d,h,l, 5b,d,f,h,j,l,n,p,r,t,v,x,z,ab,ad,af,ah,aj,al,an,ap,ar,at,av), radulae (Figure 6), general reproductive organ morphology, and inner penial wall (Figure 7a–c,e,g). Prominent folds were observed in the inner vaginal wall of *S. ishizakii*, whereas fine ventral structures were observed in the two Japanese species (Figure 7d,f,h).

3.2 | Molecular phylogenetic analyses

The 655-bp COI fragment was successfully sequenced for six *S. hirasei* (LC638865–LC638870), six *S. pallgergelyi* sp. nov. (LC638859–LC638864), three *S. ishizakii* (LC638856–LC638858), and one *S. schistoptychia* (LC638871). All *S. hirasei* snails had the same haplotype, whereas *S. ishizakii* and the new species had two different haplotypes each. In the obtained ML tree (Figure 8), each of the Japanese species appears as a strongly supported clade (BS = 100%). A well-supported clade was also formed by the Japanese species (BS = 98%). The two Japanese species had the closest relationship (1.6% K2P distance), and the K2P distances among *S. ishizakii* and the two other species were 6.7% (vs. *S. pallgergelyi* sp. nov.) and 7.0% (vs. *S. hirasei*).

3.3 | Systematics

It was suggested that a genetic distance of more than 3% is an appropriate boundary between intra- and interspecific differentiation of the COI gene (Hebert, Cywinska, Ball, & deWaard, 2003). This COI distance is generally accepted in Stylommatophora (e.g. Criscione, Law, & Köhler, 2012; Kameda, Kawakita, & Kato, 2007). However, it is also known that the interspecific distances can be as low as 1% in stylommatophoric snails (Davison, Blackie, & Scothern, 2009). In contrast, 18.4% of the genetic distances have been revealed within *Orcula dolium* (Harl, Duda, Kruckenhauser, Sattmann, & Haring, 2014). Although the genetic

255 divergence between *S. hirasei* and the new species was 1.6% and is thus lower than 3%, they
256 were clearly discriminated by their shell morphology. Their unique shell morphology and the
257 substantial difference in their habitats indicate that they adapted to their habitats upon
258 allopatric divergence and are on independent evolutionary trajectories (see Discussion).
259 Therefore, we consider *S. pallgergelyi* sp. nov. an independent species, although further
260 genetic study is needed.

261

262 Plectopylidae Möllendorff, 1898

263 Sinicolinae Páll-Gergely, 2018

264 *Sicradiscus* Páll-Gergely, 2013

265 Type species: *Plectopylis schistoptychia* Möllendorff, 1886 by original designation

266 ***Sicradiscus hirasei* (Pilsbry, 1904)**

267 Tables 2, 5; Figures 4a–d, 5a–p, 6a–c, 7c,d, 9a–c

268 *Plectopylis* (*Sinicola*) *hirasei* Pilsbry, 1904: 58–59; Minato 1980: 88–89, figures 7–10; Minato 1988: 135;

269 Azuma 1982: 210, figure 624; Azuma and Azuma 1984: 89–90, unnumbered figure (genital anatomy); Higo

270 and Goto 1993: 481; Nature Conservation Division, Department of Environmental Affairs, Okinawa

271 Prefectural Government 2017: 457.

272 *Plectopylis hirasei* – Pilsbry and Hirase 1904: 616; Iwakawa 1919: 207; Brooks and Brooks 1931: 212; Hirase

273 and Taki 1951: pl. 124, figure 6; Baker 1963: 215; Hsieh 2003: 143, unnumbered figure (adult shell).

274 *Sicradiscus hirasei* – Páll-Gergely and Hunyadi 2013: 2, 50, 57; Páll-Gergely and Asami 2014: 558–559; Páll-

275 Gergely et al. 2015b: 4, 107; Páll-Gergely 2018a: 86–89, figure 1B, C, F–H; Páll-Gergely 2018b: 105.

276

277 **Material examined.** Lectotype, ANSP 87632 (photos examined). Newly collected materials.

278 17 adult shells collected from crevices in the limestones on the ground in the inland natural

279 forest in Miyako Island, Miyakojima City, Okinawa Prefecture, Japan on 18 October 2020,

280 KUZ Z3942.

Amended diagnosis. Shell very small, lenticular, thin, dextral [D 5.8 ± 0.2 mm (mean \pm SD); H 3.0 ± 0.1 mm] with slightly keeled body whorl; apex moderately protruding (HD 0.52 ± 0.01 ; SA 138.9 ± 3.0 degrees); periostracal folds short, on dorsal side of shell (HL 0.40 mm); teleoconch surface matte, not glossy, with strong ribs and spiral striations on ventral side; parietal callus mildly elevated (CL 0.36 ± 0.06 mm); apertural fold very weak or absent; parietal wall with slightly curved and elongated anterior lamella and weaker vestigial posterior one; palatal plicae in one row, slender, rounded, and oblique; reproductive system with penial caecum; inner penial wall with longitudinal folds that form pocket-like pouches.

Measurements of lectotype. Adult shell: Measurements: BWL 2.3 mm; D 5.7 mm; H 3.0 mm; HD 0.53; SA 129.3 degrees; UD 0.39; UW 2.2 mm; WN 5.25.

Description of newly collected materials. Adult shell: Measurements are shown in Table 2. Shell lenticular, with bluntly shouldered body whorl and with conical and moderately protruding apex; light brown, translucent; 5.25–5.50 whorls separated by shallow suture; first 0.25 whorl smooth or very finely ribbed; remaining 1.75–2.00 whorl finely ribbed (Figure 4a); radial and spiral lines of comparable strength on dorsal side; same structure on the upper half of the body whorl; ventral side with stronger radial sculpture and spiral striations (Figure 4b); periostracal folds visible in fresh specimen on keel (HL 0.40 mm); umbilicus deep and wide; apertural margin thickened and strongly reflected; parietal callus mildly to strongly elevated; aperture without or with very weak fold connected to the parietal callus.

Lamellae and plicae (Figures 4c,d, 5a–p): Parietal wall with two vertical lamellae; moderately curved and elongated anterior lamella variable from near straight line to C- to T-shaped line; dorsal end of anterior one elongated anteriorly and posteriorly; weaker vestigial posterior one usually connected to anterior one; palatal plicae in one row with 6 horizontal or oblique plicae; first and sixth plicae on dorsal side small and horizontal; 6th plicae usually split in 2 horizontal parts; second longest and most slender; thick third one slender to rounded; thick, rounded, and oblique 4th and 5th rarely connected with weak prominence.

307 Radulae (Figure 6a–c): pointed central teeth same length as or slightly longer than EcL;
308 lateral tooth in 6 rows with pointed EcL, EnL, EnL 2–2.5 times longer than EcL; 8–10 row
309 marginal tooth bear pointed EcM, EnM. EnMs with incisions 1/4 to 1/6 the length of the tooth
310 2.5–3 times longer than EcM.

311 Genitalia: Atrium short; penis consisting of thicker proximal and slimmer distal portions,
312 of comparable length; internally with elevated longitudinal folds that form pocket-like
313 pouches (Figure 7c); calcareous crystals observed in penis lumen in 3 specimens of 6
314 examined ones; penial caecum well-developed, approximately half as long as proximal part of
315 penis; slender elongated retractor muscle inserts on apical part of penial caecum; epiphallus
316 joining penis laterally at base of caecum; vas deferens slender, long, distal end gradually
317 thickened to the base of spermoviduct; vagina with slightly thickened vaginal bulb, slightly
318 slender near atrium; several weak fibres attaching vaginal bulb to body wall; inner vaginal
319 wall with fine folds (Figure 7d); calcareous crystals found in vagina lumen in 2 specimens;
320 narrow stalk of the bursa copulatrix branch off from the base of spermoviduct connect to
321 elongated oval bursa copulatrix; narrow diverticulum start from slight distal portion of stalk
322 of the bursa copulatrix extends almost the same length as the end of bursa copulatrix;
323 spermoviduct long, approximately the same thickness as the proximal portion of penis; uterus
324 contained 1–5, well-developed embryo consisting of 2.5 whorls; talon relatively small;
325 albumen gland short.

326 **Remarks.** The reproductive anatomy of *S. hirasei* was first shown in Azuma and Azuma
327 (1984). Although the genital characteristics examined in that study excluded the penial
328 caecum, vaginal bulb, and diverticulum, those characters were recently described (Páll-
329 Gergely, 2018a). Reproductive organs of the newly collected snails in this study almost
330 corresponded to those in Páll-Gergely (2018a) because a penial caecum, vaginal bulb, and
331 diverticulum were present. However, the vaginal bulb was not well developed and was almost
332 as thick as the vagina.

Sicradiscus hirasei can be discriminated from *S. pallgergelyi* sp. nov. by its smaller shell with more protruding apex (larger HD, smaller SA) and less elevated parietal callus (middle CL) (Table 5). The keeled body whorl and absence of strong folds in the aperture distinguishes *S. hirasei* from the western group species of the genus and *S. transitus*. *Sicradiscus hirasei* is also distinct from *S. ishizakii* and the other continental congeners by the matte ventral side, a slightly curved and elongated anterior lamella, and palatal plicae in one row consists of rounded and oblique plicae.

***Sicradiscus ishizakii* (Kuroda, 1941)**

Tables 2, 5; Figures 4e–h, 5q–af, 6d–f, 7a,e,f,i, 9d–f

Plectopylis ishizakii Kuroda, 1941: 188–189, pl. 7 figures 42, 43; Hwang et al. 2008: 58, figure 5A–B; Nature Conservation Division, Department of Environmental Affairs, Okinawa Prefectural Government 2017: 457. *Plectopylis (Sinicola) ishizakii* – Minato 1980: 89; Chang and Ookubo 1999: 21–28, plates 1–2, figures 1–3. *Plectopylis (Chersaecia) ishizakii* – Higo and Goto 1993: 481. *Sicradiscus ishizakii* – Páll-Gergely and Hunyadi 2013: 2, 50; Páll-Gergely and Asami 2014: 558–559; Páll-Gergely et al. 2015b: 4, 107, 111; Páll-Gergely 2018a: 86–89, figure 1A, D–E; Páll-Gergely 2018b: 105.

Material examined. Paratype, NCP-244 (photos examined). Newly collected materials. 5 adult shells collected from JianShih Town, Xinzhu Country, Taiwan on 19 July 2017, KUZ Z3943. 14 adult shells collected from the same region on 29 January 1997, KUZ Z3944. 1 adult shell collected from the same region on 21 March 2017, KUZ Z3945. 1 adult shell collected from Guanxi Town, Xinzhu Country on 31 August 2017, KUZ Z3946.

Amended diagnosis. Shell small, lenticular, rather thick, dextral [D 6.5 ± 0.4 mm; H 3.1 ± 0.2 mm] with slightly keeled body whorl; apex bluntly protruding (HD 0.48 ± 0.01 ; SA 149.1 ± 3.1 degrees); periostracal folds short on dorsal side of shell (HL 0.35 ± 0.07); entire protoconch remarkably ribbed; teleoconch surface glossy, with strong ribs and without or

359 with very fine spiral striations on ventral side; callus mildly elevated ($CL\ 0.32 \pm 0.08\ mm$);
360 apertural fold absent or very weak; parietal wall with moderately curved, thick, C-shaped
361 anterior lamella and weaker vestigial posterior one; palatal plicae in one row with slender,
362 rounded, and oblique plicae; reproductive system with penial caecum; inner penial wall with
363 longitudinal folds that form pocket-like pouches.

364 **Measurements of paratype.** Adult shell: Measurements: BWL 2.7 mm; D 6.7 mm; H 3.3
365 mm; HD 0.49; SA 145.7 degrees; UD 0.39; UW 2.6 mm; WN 5.50.

366 **Description of newly collected materials.** Adult shell: Measurements are shown in Table
367 2. Shell lenticular; with bluntly keeled body whorl and with conical and slightly protruding
368 apex; pale yellow or light brown, translucent; whorls separated by shallow to medium depth
369 suture; entire protoconch remarkably ribbed (Figure 4e); dorsal side with prominent radial
370 sculpture, weak spiral lines; same structure on the upper half of the body whorl; ventral side
371 with strong radial ribs, without or with rudimental spiral striations (Figure 4f); short
372 periostracal folds visible in fresh specimens on keel (HL 0.27–0.41 mm); umbilicus deep and
373 rather narrow; apertural margin thickened and strongly reflected; parietal callus mildly
374 elevated; aperture without or with very weak fold connected to the parietal callus.

375 Lamellae and plicae (Figures 4g,h, 5q–af): Parietal wall with two vertical lamellae;
376 moderately curved, thick anterior lamella C-shaped line; dorsal end of anterior one elongated
377 anteriorly and posteriorly; weaker vestigial posterior one usually connected to anterior one;
378 palatal plicae in one row with 6 horizontal or rounded plicae; first and sixth plicae on dorsal
379 side small and horizontal; 6th plicae rarely split in 2 horizontal parts; second longest and most
380 slender; rounded, and oblique third, 4th, and 5th rarely connected with weak prominence.

381 Radulae (Figure 6d–f): pointed central teeth same length as or slightly longer than EcL;
382 lateral tooth in 7 rows with pointed EcL, EnL, EnL 2–3 times longer than EcL; 9–10 row
383 marginal tooth bear pointed EcM, EnM. EnMs with incisions 1/4 to 1/5 the length of the tooth
384 2.5–3 times longer than EcM.

Genitalia (Figure 7a,e,f,i): Atrium short; penis consisting of thicker proximal and slimmer distal portions, of comparable length; internally with elevated longitudinal folds that form pocket-like pouches; calcareous crystals observed in penis lumen in all 3 examined specimens; penial caecum well-developed, approximately half as long as proximal part of penis; slender elongated retractor muscle inserts on apical part of penial caecum; epiphallus joining penis laterally at base of caecum; vas deferens slender, long, distal end gradually thickened to the base of spermoviduct; vagina with slightly thickened vaginal bulb, slightly slender near atrium; several weak fibres attaching vaginal bulb to body wall; inner vaginal wall with prominent folds; calcareous crystals found in vagina lumen in 1 snail; narrow stalk of the bursa copulatrix branch off from the base of spermoviduct connect to elongated oval bursa copulatrix; narrow diverticulum start from slight distal portion of stalk of the bursa copulatrix extends almost the same length as the end of bursa copulatrix; spermoviduct long, approximately the same thickness as the proximal portion of penis; uterus contained 2–7, well-developed embryo consisting of 2.5 whorls; talon relatively small; albumen gland short.

Remarks. The radular morphology and reproductive anatomy of *S. ishizakii* were described by Chang and Ookubo (1999). Although there was variation in number of tooth rows was observed in this study, the radular morphology of this species was concordant with the description of the previous study.

Genital morphologies of the newly collected specimens possessed several discordances with the preceding study: i.e. there was a penial caecum and diverticulum, which were not previously found. In this study, there was a penis branched off from a vagina near the atrium; the preceding study observed a penis at a distal portion of a vagina. Prominent folds observed in the inner vaginal wall distinguished the examined *S. ishizakii* from the two other species. However, the seasonal change of the characteristics should be clarified because reproductive organ morphology has been proposed to vary relative to mating season (Páll-Gergely et al., 2015b).

Sicradiscus ishizakii can be distinguished from the other insular species by a flatter shell (smaller HD, larger SA), a less developed parietal callus (smaller CL), and a glossy ventral side (Table 5). The shell with keeled body whorl and the lack of apertural fold discriminates this species from the western group species of *Sicradiscus* and *S. transitus*. *Sicradiscus ishizakii* is also distinguishable from the other continental congeners by a moderately curved, thick, C-shaped anterior lamella and palatal plicae in one row with slender, rounded, and oblique plicae.

***Sicradiscus pallgergelyi* Sawada & Nakano, sp. nov.**

Tables 2, 5; Figures 4i–l, 5ag–av, 6g–i, 7b,g,h,j, 9g–l, 10
(New Japanese name: Yaeyama-itokakemaimai)
[urn:lsid:zoobank.org:act:E3250AC4-6494-438C-B591-1F5C99F9AA0E](https://zoobank.org/urn:lsid:zoobank.org:act:E3250AC4-6494-438C-B591-1F5C99F9AA0E)

Material examined. Holotype. KUZ Z3947, adult shell collected from gaps in fallen leaves on the ground in the inland natural forest at an elevation of around 200 meters in Iriomote Island, Taketomi Town, Yaeyama Country, Okinawa Prefecture, Japan on 15 October 2020. Paratypes. 4 specimens collected with the holotype, KUZ Z3948–Z3951. Additional materials. 20 adult specimens collected with the holotype, KUZ Z3952.

Diagnosis. Shell small, lenticular, rather thick, dextral [D 6.5 ± 0.2 mm; H 3.2 ± 0.1 mm] with bluntly keeled body whorl; apex moderately protruding (HD 0.49 ± 0.01 ; SA 144.9 ± 2.5 degrees); periostracal folds on dorsal side of shell (HL 0.38 ± 0.08 mm); teleoconch surface matte, not glossy, with strong ribs and spiral striations on ventral side; callus very strongly elevated (CL 0.44 ± 0.04 mm); apertural fold absent; Parietal wall with slightly curved and elongated anterior lamella and weaker vestigial posterior one; palatal plicae in one row with

437 rounded and oblique plicae; reproductive system with penial caecum; inner penial wall with
438 longitudinal folds that form pocket-like pouches.

439 **Description of holotype.** Adult shell (Figure 9g–i): Measurements: BWL 2.6 mm; D 6.3
440 mm; EN 6; CL 0.47 mm; H 3.1 mm; HD 0.49; SA 147.7 degrees; UD 0.39; UW 2.5 mm; WN
441 5.50. Shell lenticular; with slightly keeled body whorl and with conical and moderately
442 protruding apex; pale yellow, translucent; whorls separated by rather deep suture; first 0.25
443 whorl smooth; remaining 1.75 whorl very finely ribbed; radial and spiral lines of comparable
444 strength on dorsal side; same structure on the upper half of the body whorl; ventral side with
445 stronger radial sculpture and spiral striations; periostracal folds visible in fresh specimens on
446 keel (HL 0.42 mm); umbilicus deep and wide; apertural margin thickened and strongly
447 reflected; parietal callus very strongly elevated; aperture without fold connected to the parietal
448 callus.

449 Parietal lamellae: Not examined.

450 Palatal plicae: one row with 6 horizontal or rounded plicae; first and sixth plicae on dorsal
451 side small and horizontal; second longest, most slender, and horizontal; remaining ones thick,
452 rounded, and oblique.

453 Radula: pointed central teeth same length as or slightly longer than EcL; lateral tooth in 7
454 rows with pointed EcL, EnL, EnL 3 times longer than EcL; 9 row marginal tooth bear pointed
455 EcM, EnM. EnMs with incisions 1/5 the length of the tooth 3 times longer than EcM.

456 Genitalia: Atrium short; penis consisting of thicker proximal and slimmer distal portions,
457 of comparable length; internally with elevated longitudinal folds that form pocket-like
458 pouches; penis lumen without calcareous crystals; penial caecum well-developed,
459 approximately half as long as proximal part of penis; slender elongated retractor muscle
460 inserts on apical part of penial caecum; epiphallus joining penis laterally at base of caecum;
461 vas deferens slender, long, distal end gradually thickened to the base of spermoviduct; vagina
462 with slightly thickened vaginal bulb, slightly slender near atrium; several weak fibres

463 attaching vaginal bulb to body wall; inner vaginal wall with fine folds; vagina lumen without
464 calcareous crystals; narrow stalk of the bursa copulatrix branch off from the base of
465 spermooviduct connect to elongated oval bursa copulatrix; narrow diverticulum start from
466 slight distal portion of stalk of the bursa copulatrix extends almost the same length as the end
467 of bursa copulatrix; spermooviduct long, approximately the same thickness as the proximal
468 portion of penis; uterus contained 6, well-developed embryo consisting of 2.5 whorls; talon
469 relatively small; albumen gland short.

470 **Variation.** Adult shell (Figure 9j–l): Measurements are shown in Table 2. Shell pale
471 yellow or light to dark brown; first 0.25–0.50 whorl smooth; remaining 1.50–1.75 whorl very
472 finely ribbed; parietal callus moderately to very strongly elevated; aperture without or with
473 very weak fold connected to the parietal callus.

474 Lamellae and plicae (Figures 4k,l, 5ag–av): Parietal wall with two vertical lamellae;
475 slightly to moderately curved and elongated anterior lamella variable from near straight line
476 to C- to T-shaped line; dorsal end of weaker vestigial posterior one elongated anteriorly and
477 posteriorly and usually connected to anterior one; palatal plicae in one row with 6 horizontal
478 or rounded plicae; first and sixth plicae on dorsal side small and horizontal; second longest
479 and most slender; remaining ones thick, rounded, and oblique.

480 Radulae (Figure 6g–i): lateral tooth in 6–7 rows with pointed EcL, EnL, EnL 2–2.5 times
481 longer than EcL; 9 rows marginal tooth bear pointed EcM, EnM. EnMs with incisions 1/4 to
482 1/6 the length of the tooth 2.5–3 times longer than EcM.

483 Genitalia (Figure 7b,g,h,j): calcareous crystals found in penis lumen in 3 specimens of 8
484 examined ones; calcareous crystals found in vagina lumen in 1 specimen; uterus contained 3–
485 6, well-developed embryo consisting of 2.5 whorls.

486 **Distribution and ecology.** The new species was found from a narrow area in the interior
487 of Iriomote Island, Japan. The fossil recorded from Ishigaki Island and identified as *S. hirasei*

may belong to this species (Nature Conservation Division, Department of Environmental Affairs, Okinawa Prefectural Government, 2017).

Etymology. The specific name is dedicated to Dr. Barna Páll-Gergely, who greatly contributed to the systematics of the family Plectopylidae.

Remarks. The new species can be discriminated from *S. hirasei* by the larger shell size (larger BWL, D, H, UW) of the former species (Table 5). The new species also possesses a flatter shell (smaller HD, larger SA) and a more developed parietal callus (larger CL). Although the shell morphology of *S. pallgergelyi* sp. nov. is similar to that of *S. ishizakii* because it has a larger and flatter shell (similar values in BWL, D, H, HD, UW), the new species exhibits a more protruding apex (larger SA) and a more developed parietal callus (larger CL) than the Taiwanese species. The new species has a shell whose ventral side is not glossy, and has strong ribs and spiral striations. In contrast, the ventral side of *S. ishizakii* has a glossy appearance because it lacks spiral striae.

The matte ventral side of the new species distinguishes this species from its congeners. The new species is distinguishable from *S. feheri*, *S. mansuyi*, *S. invius*, *S. secures*, which belong to the western group of *Sicradiscus* and *S. transitus* by the presence of keeled body whorls and absence of strong folds from the aperture. The new species is also distinct from seven Chinese and Vietnamese congeners, *S. feheri*, *S. invius*, *S. cutisculptus*, *S. schistoptychia*, *S. transitus*, *S. diptychia*, *S. securus*, and *S. mansuyi* by the following internal structures: elongated and slender anterior lamella; vestigial and slender posterior lamella; and palatal plicae in one row consists of rounded and oblique plicae that are not usually connected.

4 | DISCUSSION

4.1 | Genital morphology of insular *Sicradiscus* species

The genus *Sicradiscus* has been subdivided into two species groups [based on shell characters](#) (Páll-Gergely & Hunyadi, 2013). The new species is clearly a member of the eastern group of the genus based on its slightly keeled body whorl and no fold in the aperture. Observations of reproductive organs in previous studies (Azuma and Azuma 1984, Páll-Gergely and Hunyadi 2013, Páll-Gergely and Asami 2014, Páll-Gergely et al., 2015b, Páll-Gergely 2018a) revealed that each group has different genital characteristics (Páll-Gergely 2018a). The western group species have a very weakly developed penial caecum and pockets in their inner penial wall, whereas the eastern group species have a well-developed penial caecum and parallel folds in their inner penial wall.

In the present study, the general morphology of *S. hirasei* genitalia was mostly concordant with that of Páll-Gergely (2018a) (see Remarks of *S. hirasei*). However, the previously overlooked penial caecum and diverticulum were discovered in the reproductive organs of *S. ishizakii*. The new species also possessed a clearly distinguishable penial caecum. Accordingly, it is even more likely that the members of the eastern group share the characteristics of a well-developed penial caecum, although the reproductive anatomy of *S. cutisculptus* and *S. diptychia* are still not known.

This study revealed the presence of slit-like pockets in the inner penial wall of the three examined species. In contrast to the penial caecum results, these pockets were not previously detected in the eastern group. As indicated in Páll-Gergely et al. (2015b), the inconsistencies between the present and previous observations may be due to seasonal changes because the samples were collected in different seasons [Páll-Gergely (2018a), December; this study, October]. Therefore, the inner penial wall structure is unlikely to significantly differ between the groups, and further investigation is necessary to clarify the seasonal change of these reproductive structures.

Calcareous granules were observed in the inner penial and/or vaginal wall of the three *Sicradiscus* species. It was suggested that the penial granules function as a mating apparatus

for disposable males and are lost when snails bear offspring (Páll-Gergely et al., 2015b). In this study, however, all nine individuals with granules on the inner penial wall possessed embryos, and no significant difference was detected in the number or size of embryos between the snails with or without the granules. The vaginal granules observed in the three *Sicradiscus* species have only been previously described from two other species in the family, *Halongella schlumbergeri* (Morlet, 1886) and *H. fruhstorferi* (Möllendorff, 1901). These granules have also been proposed to be seasonal and associated with mating season (Páll-Gergely et al., 2015b). In this analysis, some snails had penial and vaginal granules and some did not, even within the same population collected on the same day; this indicates that the reproductive cycle of each snail may also affect granule appearance.

4.2 | Morphological evolution of insular *Sicradiscus* species

The present morphological examination discriminated the three *Sicradiscus* species with the measurements of the apertural callus length and the spire angle. The four other quantitative characters separated *S. hirasei* from the other species. CVA based on the measurements of five characters also differentiated *S. hirasei* from *S. pallgergelyi* sp. nov. and *S. ishizakii*, which indicates that *S. hirasei* has a unique shell morphology. Moreover, *S. ishizakii* was distinguished from *S. hirasei* and the new species by the ventral sculpture of its shell and characteristics of its protoconch, lamellae, and plicae. The molecular phylogenetic analyses revealed that shell measurements of the insular *Sicradiscus* species seem to have higher plasticity than shell structure. In addition, the ventral sculpture characteristics can be estimated to be a common trait of Japanese lineages, and the Taiwanese species share characteristics with the continental congeners.

The CL measurements were largest in the new species and smallest in *S. ishizakii*. Although the function of the apertural callus is still unclear, it may help prevent natural enemies from entering the aperture if the apertural folds serve a similar function in land snails

as they do in Vertiginidae and Diapheridae (Gittenberger, 1995; Solem, 1972). In the genus *Satsuma* A. Adams, 1868, it was suggested that strong apertural folds evolved by predation pressure from snail-eating snakes of family Pareatidae in the Ryukyu Islands and Taiwan (Hoso & Hori, 2008). Even though snakes are not predators of *Sicradiscus* species due to the snails' small size, morphological evolution in the apertural callus may be promoted by predation pressures from snail-eating fireflies, which occur on each of the Ryukyu Islands (Ohba, 2004). The relationship between aperture size and water loss revealed that the apertural callus may also prevent water loss from the aperture by reducing the amount of air that passes through the aperture (Machin, 1967).

The proportion of shell height to shell diameter of *S. hirasei* found from gaps in limestone was larger than that of the new species, which was found in gaps in fallen leaves on the ground. Land snails with a low-spired shell tend to prefer low-angle or horizontal surfaces, whereas the species with intermediate shell shapes are active on a wide variety of angles (Cain & Cowie, 1978; Cameron, 1978). It was also theorized that a low-spired shell is well-balanced in both horizontal and vertical substrates (Okajima & Chiba, 2009). In addition, it is known that a flat shell morphology is more advantageous in narrow spaces such as rock crevices (Goodfriend, 1986). Because *Sicradiscus* species are small, it is unclear whether shell balance significantly contributes to shell morphology. However, the present results of the larger HD of the rock dweller may be explained by their habitat use: *S. hirasei* is active on rocks with various angular conditions, whereas the other species are restricted to the vicinity of the horizontal ground. It was also shown that land snails in limestone areas tend to thicken their shells in response to calcium availability (Owen 1965), although the *S. hirasei* shells were the thinnest among the three species. Because shell thickness is also related to predation pressure (Moreno-Rueda, 2009), different predation pressures among islands may potentially affect the shell thickness of *Sicradiscus* species.

The two Japanese species are phylogenetically closely related, which indicates that major morphological shifts occurred in the two species, even though *Sicradiscus* species are estimated to experienced only slight conchological changes (Páll-Gergely & Hunyadi, 2013). The aforementioned morphological differences between *S. hirasei* and the new species strongly indicates that the common ancestor of the Japanese lineage expanded to different islands and underwent different selection pressures, which resulted in speciation.

4.3 | Radular morphology

The radular morphology of *Sicradiscus* was examined in *S. ishizakii* and four other species by Chang and Ookubo (1999) and Páll-Gergely et al. (2015b), and the latter study also reported that the shape of the radulae was highly preserved among related genera. In this examination, significant differences were not observed in radular morphology among the three *Sicradiscus* species, and the *S. ishizakii* radulae corresponded to those described by Chang and Ookubo (1999). The radulae of the three species consisted of a relatively large central tooth, a lateral tooth with ectocones as large as cusps of a central tooth, and tricuspid marginal teeth with pointed cusps and deep incisions between the cusps; these characteristics are similar to those of the radulae of other congeners and members of *Sinicola* and *Gudeodiscus* (Páll-Gergely et al., 2015b).

4.4 | Taxonomic position of other insular populations of *Sicradiscus*

The new species was discovered in a well-preserved natural forest at an elevation of approximately 200 m on Iriomote Island. In addition to the record on the island, fossil specimens previously identified as *S. hirasei* were found on Ishigaki Island between Miyako Island and Taiwan (Nature Conservation Division, Department of Environmental Affairs, Okinawa Prefectural Government, 2017). Although only fossil specimens have been collected from Ishigaki Island, extant *Sicradiscus* snails may be distributed on the island because the

natural forests are preserved on the island and are similar to the habitat of the new species. Taking into account the similarity of the land snail faunas between the two islands (Habe & Chinen, 1974), the fossil records on Ishigaki Island likely belong to *S. pallgergelyi* sp. nov.

The length of the apertural callus distinguishes the three insular species. Although the apertural structure may facilitate self-protection, a population without callus was also found in central Taiwan (Lee & Chen, 2003). This population also has a smaller number of ribs on the ventral side of the shell compared with *S. ishizakii* of northern Taiwan and the Japanese species. Because there are other species in northern and central Taiwan (Hsieh, 2003) and the length of the callus may be related to different selection pressures, this central population may be an independent species with a unique evolutionary history. The systematic position of the populations in Ishigaki Island and central Taiwan should be examined in future studies.

Acknowledgements

We are very grateful to Dr. Barna Páll-Gergely (Plant Protection Institute, Centre for Agricultural Research) for providing materials and helpful comments on our manuscript. We also thank two anonymous reviewers for their constructive comments on the manuscript. We are also grateful to Miyakojima City for providing permission for *Sicradiscus* sample collection. We also thank Jamen Uiriamu Otani, Taiji Kurozumi, Takashi Hosoda, and Kanji Ookubo for providing information on *Sicradiscus*. The first author is grateful to Jamen Uiriamu Otani, Yuji Nakahara, Wei Lin, Dr. Yuta Morii (Kyoto University; KU), Tatsuki Nishioka (KU), and Iriomote Station of Ryukyu University, Japan for assisting with sample collection. The first author also thanks Dr. Taku Okamoto, Tomohisa Makino, Yusuke Sugawara, Tomoki Kadokawa, Professor Minoru Tamura (KU), and Dr. Takahiro Hirano (Tohoku University) for supporting SEM observations, preparation of the figure of the map, and morphological and phylogenetic analyses. This study was financially supported in part by

643 JSPS KAKENHI Grant Number JP21J22917 and the Tokyo Metropolitan University Fund for
644 TMU Strategic Research (Leader: Professor Noriaki Murakami at TMU; FY2020–FY2022).
645 We thank Dr. Eckstut Mallory (Edanz) for editing a draft of this manuscript.

646 **References**

- 647 Azuma, M. (1982). *Coloured illustrations of the land snails of Japan*. Hoikusha, Osaka.
- 648 Azuma, M., & Azuma, Y. (1984). Distribution of land snails of Miyako Islands, the South-
649 western Okinawa, Japan (1st report). *Satsuki*, 20, 85–98.
- 650 Baker, H. B. (1963). Type land snails in the Academy of Natural Sciences of Philadelphia
651 Part II. Land Pulmonata, exclusive of North America North of Mexico. *Proceedings of*
652 *the Academy of Natural Sciences of Philadelphia*, 115, 191–259.
- 653 Brooks, S. T., & Brooks, B. W. (1931). List of types of Amphineura and Gastropoda in the
654 collection of the Carnegie Museum. *Annals of the Carnegie Museum*, 20(2), 179–253.
- 655 Cain, A., & Cowie, R. (1978). Activity of different species of land-snail on surfaces of
656 different inclinations. *Journal of Conchology*, 29, 267–272.
- 657 Cameron, R. A. D. (1978). Differences in the sites of activity of coexisting species of land
658 mollusc. *Journal of Conchology*, 29, 273–278.
- 659 Chang, K. M., & Ookubo, K. (1999). Anatomy and systematics on *Plectopylis* (*Sinicola*)
660 *ishizakii* Kuroda, 1941 from Taiwan. *Bulletin of Malacology*, 23, 21–28.
- 661 Criscione, F., Law, M., & Köhler, F. (2012). Land snail diversity in the monsoon tropics of
662 Northern Australia: Revision of the genus *Exiligada* Iredale, 1939 (Mollusca:
663 Pulmonata: Camaenidae), with description of 13 new species. *Zoological Journal of the*
664 *Linnean Society*, 166, 689–722. doi.org/10.1111/j.1096-3642.2012.00863.x
- 665 Davison, A., Blackie, R. L. E., & Scothern, G. P. (2009). DNA barcoding of
666 stylommatophoran land snails: a test of existing sequences. *Molecular Ecology*
667 *Resources*, 9(4), 1092–1101. doi.org/https://doi.org/10.1111/j.1755-0998.2009.02559.x
- 668 Folmer, O., Black, M. B., Hoeh, W., Lutz, R., & Vrijenhoek, R. (1994). DNA primers for
669 amplification of mitochondrial Cytochrome C oxidase subunit I from diverse metazoan
670 invertebrates. *Molecular Marine Biology and Biotechnology*, 3, 294–299.

671 Gittenberger, E. (1995). Adaptations of the aperture in terrestrial gastropod-pulmonate shells.
 672 *Netherlands Journal of Zoology*, 46, 191–205. doi.org/10.1163/156854295X00159
 673 Goodfriend, G. A. (1986). Variation in land-snail shell form and size and its causes: a review.
 674 *Systematic Biology*, 35(2), 204–223. doi.org/10.1093/sysbio/35.2.204
 675 Gude, G. K. (1899). Armature of Helicoid landshells and new sections of *Plectopylis*. *Science*
 676 *Gossip*, 6, 147–149.
 677 Habe, T., & Chinen, M. (1974). Land molluscan fauna of Ishigaki and Iriomote Islands, with
 678 notes on biogeography of Ryukyu Archipelago. *Memoirs of the National Museum of*
 679 *Nature and Science*, 7, 121–128.
 680 Hammer, O., Harper, D., & Ryan, P. (2001). PAST: paleontological statistics software
 681 package for education and data analysis. *Palaeontologia Electronica*, 4, 1–9.
 682 Harl, J., Duda, M., Kruckenhauser, L., Sattmann, H., & Haring, E. (2014). In Search of
 683 Glacial Refuges of the Land Snail *Orcula dolium* (Pulmonata, Orculidae) - An
 684 Integrative Approach Using DNA Sequence and Fossil Data. *PLOS ONE*, 9(5): e96012.
 685 doi.org/10.1371/journal.pone.0096012
 686 Hebert, P. D. N., Cywinska, A., Ball, S. L., & deWaard, J. R. (2003). Biological
 687 identifications through DNA barcodes. *Proceedings of the Royal Society of London.*
 688 *Series B: Biological Sciences*, 270(1512), 313–321. doi.org/10.1098/rspb.2002.2218
 689 Higo, S., & Goto, Y. (1993). *A systematic list of molluscan shells from the Japanese Is. and*
 690 *the adjacent area*. Elle Scientific Publications, Yao.
 691 Hirase, S., & Taki, I. (1951). *An illustrated handbook of shells in natural colors from the*
 692 *Japanese Islands and adjacent territory*. Bunkyoakaku, Tokyo.
 693 Hosoi, M., & Hori, M. (2008). Divergent shell shape as an antipredator adaptation in tropical
 694 land snails. *The American Naturalist*, 172(5), 726–732. doi.org/10.1086/591681
 695 Hsieh, B. C. (2003). *Landsnails of Taiwan*. Forestry Bureau Council of Agriculture, Taipei.

696 Hwang, C. C., Wu, S. P., Ohara, K., Otani, Y., & Otani, J. U. (2008). Further land snail types
 697 collected from Taiwan and deposited in the Nishinomiya Shell Museum. *Venus*, 67(1–2),
 698 53–60. doi.org/10.18941/venus.67.1-2_53
 699 Iwakawa, T. (1919). *Catalogue of Japanese Mollusca in the Natural History Department*,
 700 *Tokyo Imperial Museum*, Tokyo imperial museum, Tokyo.
 701 Kameda, Y., Kawakita, A., & Kato, M. (2007). Cryptic genetic divergence and associated
 702 morphological differentiation in the arboreal land snail *Satsuma (Luchuhadra)*
 703 *largillierti* (Camaenidae) endemic to the Ryukyu Archipelago, Japan. *Molecular*
 704 *Phylogenetics and Evolution*, 45(2), 519–533.
 705 doi.org/https://doi.org/10.1016/j.ympev.2007.03.021
 706 Kuroda, T. (1941). A catalogue of molluscan shells from Taiwan (Formosa), with description
 707 of new species. *Memoirs of the Faculty of Science and Agriculture, Taihoku Imperial*
 708 *University*, 22, 65–216.
 709 Lee, Y. J., & Chen, W. D. (2003). *Nature encyclopedia 3: land snail*. KissNature, Taipei.
 710 Machin, J. (1967). Structural adaptation for reducing water-loss in three species of terrestrial
 711 snail. *Journal of Zoology*, 152, 55–65. doi.org/10.1111/j.1469-7998.1967.tb01638.x
 712 Minato, H. (1980). Land shell fauna of Miyako Islands, the southern Ryukyu, Japan. *Venus*,
 713 39(2), 83–99.
 714 Minato, H. (1988). *A systematic and bibliographic list of the Japanese land snails*. Society for
 715 the publication of a systematic and bibliographic list of the Japanese land snails,
 716 Shirahama.
 717 Möllendorff, O. F. (1898). Verzeichniss der auf den Philippinen lebenden landmollusken.
 718 *Abhandlungen Der Naturforschenden Gesellschaft Zu Görlitz*, 22, 25–208.
 719 Möllendorff, O. F. von. (1886). Materialien zur fauna von China. *Jahrbücher Der Deutschen*
 720 *Malakozoologischen Gesellschaft*, 13, 156–210.

721 MolluscaBase eds. (2021). MolluscaBase. Plectopylidae Möllendorff, 1898. Retrieved from
 722 <http://www.molluscabase.org/aphia.php?p=taxdetails&id=870142>.
 723 Moreno-Rueda, G. (2009). Disruptive selection by predation offsets stabilizing selection on
 724 shell morphology in the land snail *Iberus g. gualtieranus*. *Evolutionary Ecology*, 23,
 725 463–471. doi.org/10.1007/s10682-008-9245-5
 726 Nature Conservation Division, Department of Environmental Affairs, Okinawa Prefectural
 727 Government. (2017). *Threatened wildlife in Okinawa, third edition (animals)—red data*
 728 *okinawa*—. Nature Conservation Division, Department of Environmental Affairs,
 729 Okinawa Prefectural Government, Naha.
 730 Nguyen, L. T., Schmidt, H. A., von Haeseler, A., & Minh, B. Q. (2015). IQ-TREE: a fast and
 731 effective stochastic algorithm for estimating maximum-likelihood phylogenies.
 732 *Molecular Biology and Evolution*, 32(1), 268–274. doi.org/10.1093/molbev/msu300
 733 Ohba, N. (2004). *Mystery of fireflies*. Yokosuka City Museum, Yokosuka.
 734 Okajima, R., & Chiba, S. (2009). Cause of bimodal distribution in the shape of a terrestrial
 735 gastropod. *Evolution*, 63(11), 2877–2887. doi.org/10.1111/j.1558-5646.2009.00780.x
 736 Okamoto, T., & Hikida, T. (2009). Three genetic lineages of the Japanese skink *Plestiodon*
 737 *japonicus* (Scincidae, Squamata) and the genetic composition of their contact zones.
 738 *Journal of Zoological Systematics and Evolutionary Research*, 47(2), 181–188.
 739 doi.org/10.1111/j.1439-0469.2008.00513.x
 740 Okamoto, Taku, Motokawa, J., Toda, M., & Hikida, T. (2006). Parapatric distribution of the
 741 lizards *Plestiodon* (formerly *Eumeces*) *latiscutatus* and *P. japonicus* (Reptilia: Scincidae)
 742 around the Izu Peninsula, Central Japan, and its biogeographic implications. *Zoological*
 743 *Science*, 23(5), 419–425. doi.org/10.2108/zsj.23.419
 744 Owen, D. F. (1965). A population study of an equatorial land snail, *Limicolaria martensiana*
 745 (Achatinidae). *Proceedings of the Zoological Society of London*, 144(3), 361–382.
 746 doi.org/10.1111/j.1469-7998.1965.tb05188.x

747 Páll-Gergely, B. (2018a). Redescription of the reproductive anatomy and the plication of
 748 *Sicradiscus hirasei* (Pilsbry, 1904) (Gastropoda: Pulmonata: Plectopylidae). *Venus*,
 749 76(1–4), 86–89. doi.org/10.18941/venus.76.1-4_86
 750 Páll-Gergely, B. (2018b). Systematic revision of the Plectopylinae (Gastropoda, Pulmonata,
 751 Plectopylidae). *European Journal of Taxonomy*, 455, 1–114.
 752 doi.org/10.5852/ejt.2018.455
 753 Páll-Gergely, B., & Asami, T. (2014). Additional information on the distribution, anatomy
 754 and systematics of living and fossil Chinese Plectopylidae (Gastropoda: Pulmonata).
 755 *Genus*, 25, 527–564.
 756 Páll-Gergely, B., Budha, P., Naggs, F., Backeljau, T., & Asami, T. (2015a). Review of the
 757 genus *Endothyrella* Zilch, 1960 with description of five new species (Gastropoda,
 758 Pulmonata, Plectopylidae). *ZooKeys*, 529, 1–70. doi.org/10.3897/zookeys.529.6139
 759 Páll-Gergely, B., & Hunyadi, A. (2013). The family Plectopylidae Möllendorff 1898 in China
 760 (Gastropoda, Pulmonata). *Archiv Für Molluskenkunde International Journal of*
 761 *Malacology*, 142, 1–66. doi.org/10.1127/arch.moll/1869-0963/142/001-066
 762 Páll-Gergely, B., Hunyadi, A., Ablett, J., Luong Van, H., Naggs, F., & Asami, T. (2015b).
 763 Systematics of the family Plectopylidae in Vietnam with additional information on
 764 Chinese taxa (Gastropoda, Pulmonata, Stylommatophora). *ZooKeys*, 473, 1–118.
 765 doi.org/10.3897/zookeys.473.8659
 766 Páll-Gergely, B., Muratov, I., & Asami, T. (2016). The family Plectopylidae (Gastropoda,
 767 Pulmonata) in Laos with the description of two new genera and a new species. *ZooKeys*,
 768 592, 1–26. doi.org/10.3897/zookeys.592.8118
 769 Pilsbry, H. A. (1904). *Plectopylis* in the Riukiu Islands. *Nautilus*, 18(3), 58–59.
 770 Pilsbry, H. A., & Hirase, Y. (1904). Descriptions of new land snails of the Japanese Empire.
 771 *Proceedings of the Academy of Natural Sciences of Philadelphia.*, 56, 616–638.

772 Sawada, N., & Nakano, T. (2021). Revisiting a 135-year-old taxonomic account of the
773 freshwater snail *Semisulcospira multigranosa*: designating its lectotype and describing a
774 new species of the genus (Mollusca: Gastropoda: Semisulcospiridae). *Zoological*
775 *Studies*, 60, 7. doi:10.6620/ZS.2021.60-07

776 Schneider, C. A., Rasband, W. S., & Eliceiri, K. W. (2012). NIH image to ImageJ: 25 years of
777 image analysis. *Nature Methods*, 9(7), 671–675. doi.org/10.1038/nmeth.2089

778 Solem, A. (1972). Microarmature and barriers in the aperture of land snails. *Veliger*, 15, 81–
779 87.

780 Stecher, G., Tamura, K., & Kumar, S. (2020). Molecular Evolutionary Genetics Analysis
781 (MEGA) for macOS. *Molecular Biology and Evolution*, 37(4), 1237–1239.
782 doi.org/10.1093/molbev/msz312

783

784 Figure legends

785 FIGURE 1 Map of Ryukyu Islands and Taiwan showing sampling localities of *Sicradiscus*
786 species: green circle, *Sicradiscus hirasei*; blue triangle, *Sicradiscus ishizakii*; red square,
787 *Sicradiscus pallgergelyi* sp. nov.

788

789 FIGURE 2 Schematic drawings of shell measurements used to examine *Sicradiscus* species in
790 this study. (a) Lateral side of an adult shell. (b) Ventral side of an adult shell.
791 Measurement abbreviations: BWL, body whorl length; D, shell diameter; H, shell height;
792 SA, spire angle; UW, umbilicus width

793

794 FIGURE 3 Scatter plot of canonical variate 1 versus canonical variate 2

795

796 FIGURE 4 Protoconchs, adult shell sculptures of the ventral side, parietal lamellae, and
797 palatal plicae of *Sicradiscus* species. (a), (e), (i) Protoconch. (b), (f), (j) Shell sculptures.
798 (c), (g), (k) Parietal lamellae. (d), (h), (l) Palatal plicae. (a)–(d) *Sicradiscus hirasei* KUZ
799 Z3942. (e)–(h) *Sicradiscus ishizakii* KUZ Z3943, Z3944. (i)–(l) *Sicradiscus pallgergelyi*
800 sp. nov. KUZ Z3950, Z3952. Scale bars: (a), (d), (e), (h), (i), (l) 1000 μm ; (b), (c), (d),
801 (f), (g), (j), (k) 500 μm

802

803 FIGURE 5 Parietal and palatal plication of *Sicradiscus* species. (a), (c), (e), (g), (i), (k), (m),
804 (o), (q), (s), (t), (u), (w), (y), (aa), (ac), (ae), (ag), (ai), (ak), (am), (ao), (aq), (as), (au),
805 Parietal lamellae. (b), (d), (f), (h), (j), (l), (n), (p), (r), (t), (v), (x), (z), (ab), (ad), (af),
806 (ah), (aj), (al), (an), (ap), (ar), (at), (av), Palatal plicae. (a)–(p), *Sicradiscus hirasei*, KUZ
807 Z3942. (q)–(af), *Sicradiscus ishizakii*, KUZ Z3943–Z3944. (ag)–(av), *Sicradiscus*
808 *pallgergelyi* sp. nov., KUZ Z3950, Z3952. Aperture direction is indicated under (a) and
809 (b). Gray drawings represent vestigial parts of lamellae

810

811 FIGURE 6 Radulae of *Sicradiscus* species. (a), (d), (g) Middle parts of radulae. (b), (e), (h)
812 Central and lateral teeth. (c), (f), (i) Lateral teeth. (a)–(c) *Sicradiscus hirasei* KUZ
813 Z3942. (d)–(f) *Sicradiscus ishizakii* KUZ Z3943. (g)–(i) *Sicradiscus pallgergelyi* sp.
814 nov. KUZ Z3952. Scale bars: (a), (d), (g) 100 μ m; (b), (c), (e), (f), (h), (i) 50 μ m

815

816 FIGURE 7 Reproductive anatomy of *Sicradiscus* species. (a), (b) Reproductive system. (c),
817 (e), (g) Inner penial wall. (d), (f), (f) Inner vaginal wall. (i), (j) Embryo. (a), (e), (f), (i)
818 *Sicradiscus ishizakii*, KUZ Z3943. (b), (g), (h), (j) *Sicradiscus pallgergelyi* sp. nov.,
819 KUZ Z3949 (c), (d) *Sicradiscus hirasei*, KUZ Z3942. Atria are on the upper side of
820 the images of (c)–(h). Abbreviations: A, atrium; AG, albumen gland; B, bursa of the
821 bursa copulatrix; BS, stalk of bursa copulatrix; D, diverticulum; E, epiphallus; EM,
822 embryo; P, penis; PC, penial caecum; RM, retractor muscle; SO, spermoviduct; T, talon;
823 U, uterus; V, vagina; VB, vaginal bulb; VD, vas deferens. Scale bars: (a), (b), (i), (j)
824 1000 μ m; (c)–(h) 200 μ m

825

826 FIGURE 8 Maximum likelihood tree built from COI DNA barcodes of three insular
827 *Sicradiscus* species and *S. schistoptychia* (the type species of *Sicradiscus*). Numbers on
828 nodes represent bootstrap values

829

830 FIGURE 9 Adult shells of *Sicradiscus* species. (a)–(c) *Sicradiscus hirasei* KUZ Z3942. (d)–
831 (f) *Sicradiscus ishizakii* KUZ Z3943. (g)–(l) *Sicradiscus pallgergelyi* sp. nov. (g)–(i)
832 Holotype, KUZ Z3947. (j)–(l) Paratype, KUZ Z3949. Scale bar: 2 mm

833

834 FIGURE 10 Living specimen of *Sicradiscus pallgergelyi* sp. nov. Scale bar: 1 mm.

835 TABLE 1 Specimen list with voucher numbers, collection localities. INSD accession numbers
836 for COI sequences are also provided for specimens used for phylogenetic analysis. All
837 sequences were newly obtained in the present study. KUZ, Zoological Collection of Kyoto
838 University;

Taxon	Voucher #	Collection locality	INSD accession #
Ingroup			
<i>Sicradiscus hirasei</i>			
HM04, 08–17	KUZ Z3942	Miyakojima City in Miyako Island, Japan	
HM01	KUZ Z3990	Miyakojima City in Miyako Island, Japan	LC638865
HM02	KUZ Z3991	Miyakojima City in Miyako Island, Japan	LC638866
HM03	KUZ Z3992	Miyakojima City in Miyako Island, Japan	LC638867
HM05	KUZ Z3993	Miyakojima City in Miyako Island, Japan	LC638868
HM06	KUZ Z3994	Miyakojima City in Miyako Island, Japan	LC638869
HM07	KUZ Z3995	Miyakojima City in Miyako Island, Japan	LC638870
<i>Sicradiscus ishizakii</i>			
IT04–05	KUZ Z3943	JianShih Town, Xinzhu County, Taiwan	
IT06–19	KUZ Z3944	JianShih Town, Xinzhu County, Taiwan	
IT20	KUZ Z3945	JianShih Town, Xinzhu County, Taiwan	
IT21	KUZ Z3946	JianShih Town, Xinzhu County, Taiwan	
IT01	KUZ Z3996	JianShih Town, Xinzhu County, Taiwan	LC638856
IT02	KUZ Z3997	JianShih Town, Xinzhu County, Taiwan	LC638857
IT03	KUZ Z3998	Guanxi Town, Xinzhu County, Taiwan	LC638858
<i>S. pallgergelyi</i> sp. nov.			
SI25	KUZ Z3947 (holotype)	Taketomi Town in Iriomote Island, Japan	
SI06	KUZ Z3948 (paratype)	Taketomi Town in Iriomote Island, Japan	LC638862
SI19	KUZ Z3949 (paratype)	Taketomi Town in Iriomote Island, Japan	
SI21	KUZ Z3950 (paratype)	Taketomi Town in Iriomote Island, Japan	
SI23	KUZ Z3951 (paratype)	Taketomi Town in Iriomote Island, Japan	
SI01, 05, 09–18, 20, 22, 24	KUZ Z3952	Taketomi Town in Iriomote Island, Japan	
SI02	KUZ Z3999	Taketomi Town in Iriomote Island, Japan	LC638859

SI03	KUZ Z4000	Taketomi Town in Iriomote Island, Japan	LC638860
SI04	KUZ Z4001	Taketomi Town in Iriomote Island, Japan	LC638861
SI07	KUZ Z4002	Taketomi Town in Iriomote Island, Japan	LC638863
SI08	KUZ Z4003	Taketomi Town in Iriomote Island, Japan	LC638864
<hr/>			
Outgroup			
<hr/>			
<i>Sicradiscus</i>			
<i>schistoptychia</i>			
<hr/>			
SC01		Jiuyi National Park, Ningyuan Country, Yongzhou, Hunan, China	LC638871
<hr/>			

839

840

841 TABLE 2 Morphometric characters and number of specimens of the three *Sicradiscus* species
842 examined in this study. Measurements and counts: minimum–maximum value (mean \pm SD)

Number / Characters	<i>S. hirasei</i>	<i>S. ishizakii</i>	<i>S. pallgergelyi</i> sp. nov.
number of specimen examined (CL/EN/HL/other characters)	10 / 6 / 1 / 17	12 / 3 / 3 / 21	12 / 8 / 3 / 25
body whorl length (BWL, mm)	2.2–2.5 (2.4 \pm 0.1)	2.4–2.9 (2.6 \pm 0.2)	2.4–2.7 (2.6 \pm 0.1)
apertural callus length (CL, mm)	0.30–0.51 (0.36 \pm 0.06)	0.17–0.43 (0.32 \pm 0.08)	0.35–0.54 (0.44 \pm 0.04)
shell diameter (D, mm)	5.4–6.2 (5.8 \pm 0.2)	5.7–7.2 (6.5 \pm 0.4)	6.2–6.9 (6.5 \pm 0.2)
embryo number (EN)	EN 1–5 (3.0 \pm 1.5)	EN 2–7 (4.7 \pm 2.5)	3–6 (4.3 \pm 1.3)
shell height (H, mm)	2.8–3.3 (3.0 \pm 0.1)	2.8–3.6 (3.1 \pm 0.2)	3.1–3.4 (3.2 \pm 0.1)
Hair length (HL, mm)	0.40	0.27–0.41 (0.35 \pm 0.07)	0.29–0.42 (0.38 \pm 0.08)
the proportion of shell height to shell diameter (HD)	0.50–0.55 (0.52 \pm 0.01)	0.45–0.50 (0.48 \pm 0.01)	0.45–0.52 (0.49 \pm 0.01)
spire angle (SA, degrees)	132.9–143.2 (138.9 \pm 3.0)	142.9–154.2 (149.1 \pm 3.1)	139.1–150.4 (144.9 \pm 2.5)
the proportion of umbilicus width to shell diameter (UD)	0.35–0.39 (0.37 \pm 0.01)	0.36–0.40 (0.38 \pm 0.01)	0.36–0.43 (0.39 \pm 0.02)
umbilicus width (UW, mm)	2.0–2.4 (2.2 \pm 0.1)	2.1–2.8 (2.5 \pm 0.2)	2.2–2.9 (2.5 \pm 0.2)
whorl number (WN)	5.25–5.50 (5.3 \pm 0.1)	5.00–5.50 (5.3 \pm 0.2)	5.00–5.50 (5.3 \pm 0.2)

843

844

845 TABLE 3 Primer sequence specifications used for the polymerase chain reaction.

Primers	Sequences (5' to 3')	Origin
LCO149	GGTCAACAAATCATAAAGATAT	Folmer, Black, Hoeh, Lutz & Vrijenhoek (1994)
0	TGG	
HCO21	TAAACTTCAGGGTGACCAAAAA	Folmer et al. (1994)
98	ATCA	

846

847

848 TABLE 4 Eigenvalues, percent of explained variance, cumulated percent of explained
849 variance for the two canonical variates (CV), and the contribution of each variable to the
850 components

	CV1	CV2
Eigenvalue	4.72	0.49
Percent of explained variance	90.5	9.5
Cumulated percent of explained variance	90.5	100.0
Contributions of the variables to the factors:		
apertural callus length	-0.18	-1.36
shell diameter	1.15	-1.85
shell height	0.26	1.40
spire angle	1.41	0.99
whorl number	-0.37	0.20

851
852

853 TABLE 5 Comparison of morphological characters between the three *Sicradiscus* species
854 examined in this study. Measurements show mean \pm SD.

Characters	<i>S. hirasei</i>	<i>S. ishizakii</i>	<i>S. pallgergelyi</i> sp. nov.
body whorl length (BWL, mm)	small (2.4 ± 0.1)	large (2.6 ± 0.2)	large (2.6 ± 0.1)
apertural callus length (CL, mm)	middle (0.36 ± 0.06)	short (0.32 ± 0.08)	long (0.44 ± 0.04)
shell diameter (D, mm)	small (5.8 ± 0.2)	large (6.5 ± 0.4)	large (6.5 ± 0.2)
the proportion of shell height to shell diameter (HD)	large (0.52 ± 0.01)	small (0.48 ± 0.01)	small (0.49 ± 0.01)
spire angle (SA, degrees)	small (138.9 ± 3.0)	large (149.1 ± 3.1)	middle (144.9 ± 2.5)
umbilicus width (UW, mm)	small (2.2 ± 0.1)	large (2.5 ± 0.2)	large (2.5 ± 0.2)
surface of the protoconch	smooth or very finely ribbed	remarkably ribbed	smooth or very finely ribbed
gloss of the shell ventral side	absent	present	absent
microstructure of the shell ventral side	both spiral and radial striations	only radial striations	both spiral and radial striations
anterior lamellae	narrow, elongated, T-shaped	thick, C-shaped	narrow, elongated, T-shaped

855

856

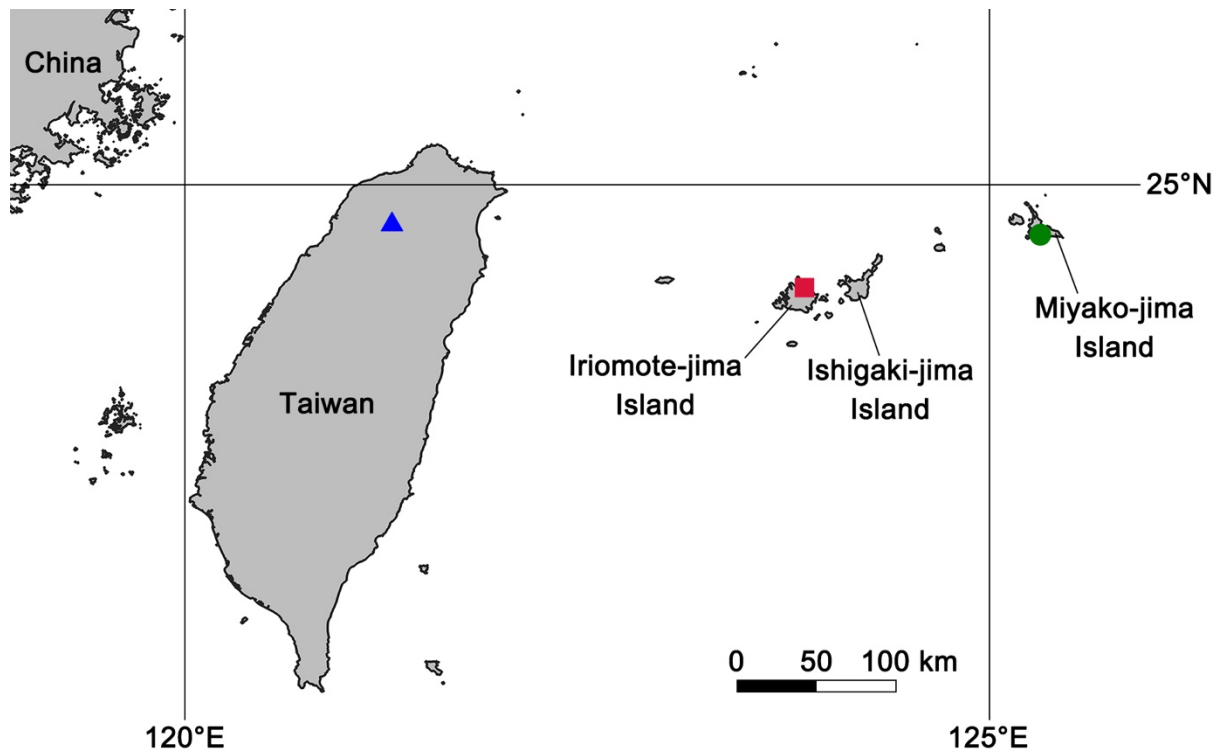
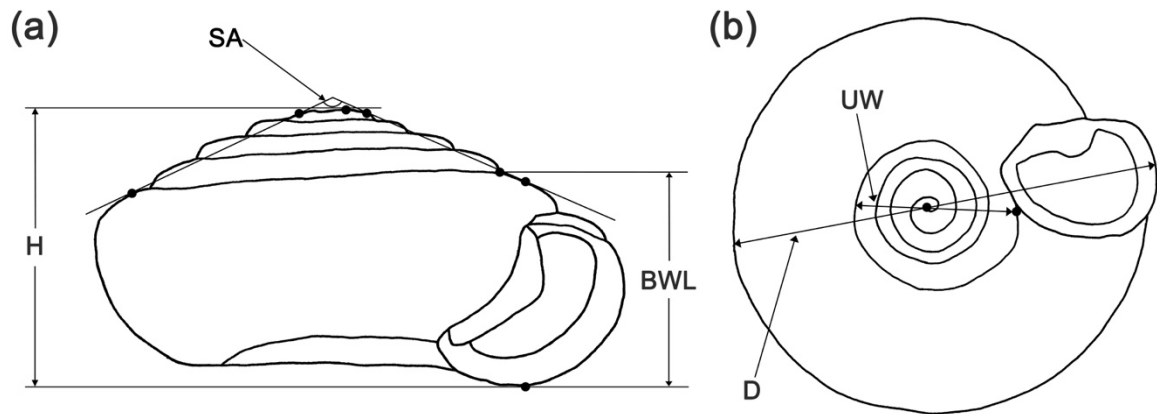


FIGURE 1 Map of Ryukyu Islands and Taiwan showing sampling localities of *Sicradiscus* species: green circle, *Sicradiscus hirasei*; blue triangle, *Sicradiscus ishizakii*; red square, *Sicradiscus pallgergelyi* sp. nov.



862

863 FIGURE 2 Schematic drawings of shell measurements used to examine *Sicradiscus* species in
 864 this study. (a) Lateral side of an adult shell. (b) Ventral side of an adult shell. Measurement
 865 abbreviations: BWL, body whorl length; D, shell diameter; H, shell height; SA, spire angle;
 866 UW, umbilicus width

867

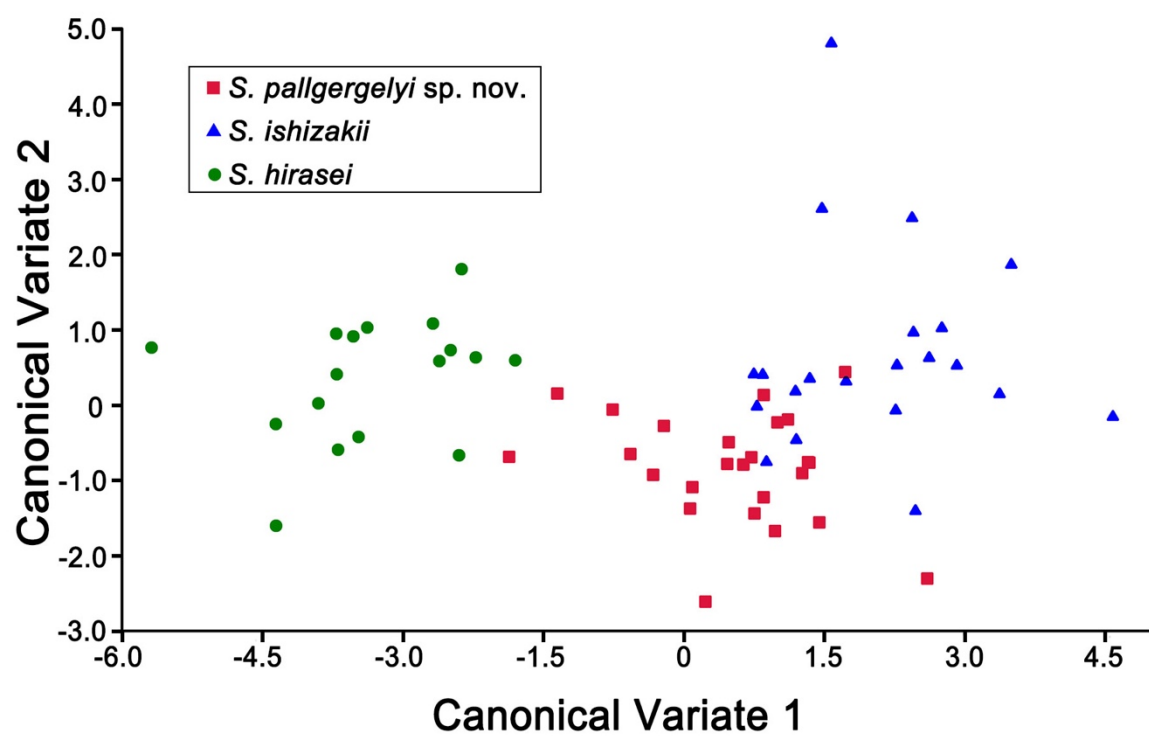


FIGURE 3 Scatter plot of canonical variate 1 versus canonical variate 2

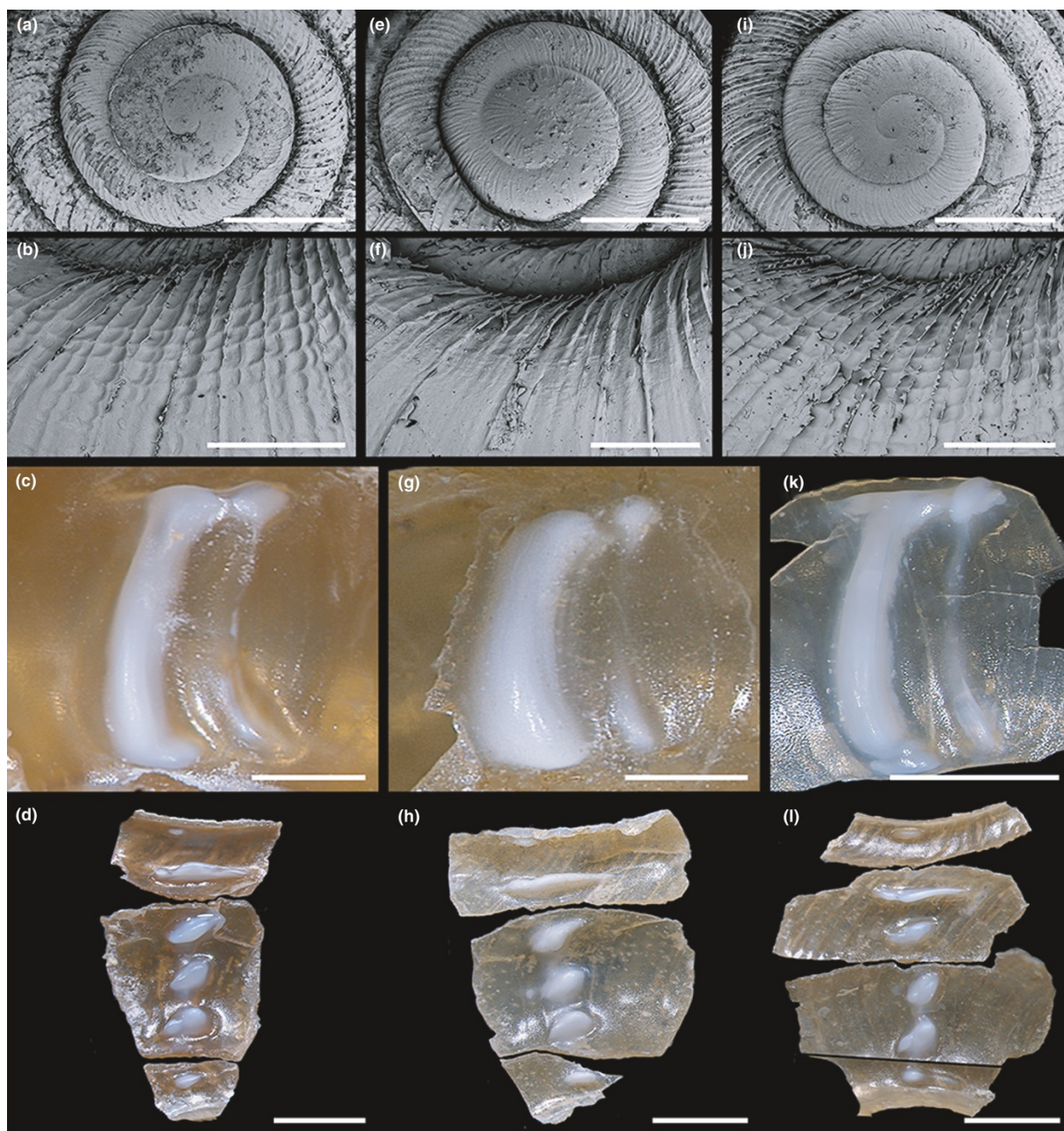
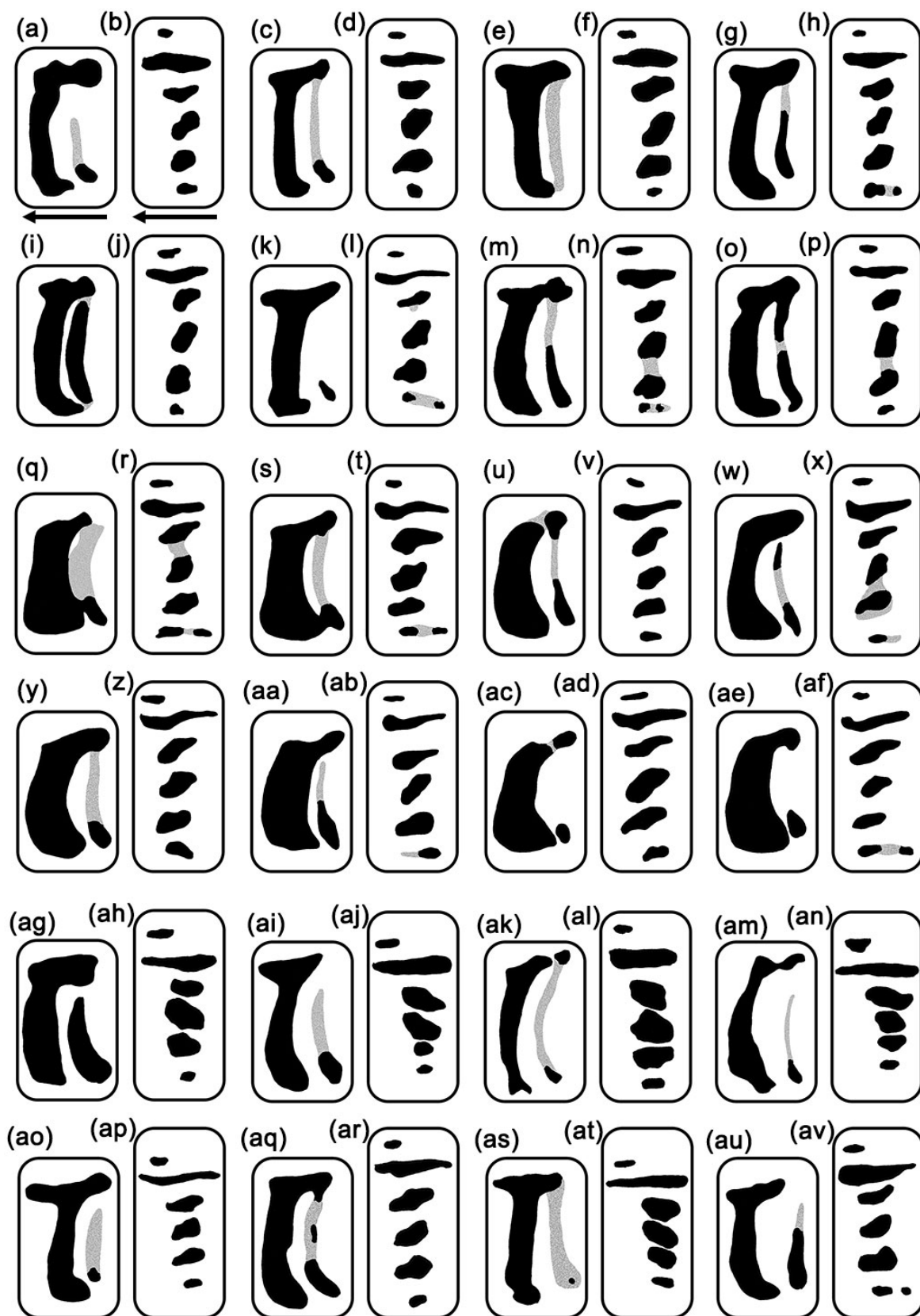


FIGURE 4 Protoconchs, adult shell sculptures of the ventral side, parietal lamellae, and palatal plicae of *Sicradiscus* species. (a), (e), (i) Protoconch. (b), (f), (j) Shell sculptures. (c), (g), (k) Parietal lamellae. (d), (h), (l) Palatal plicae. (a)–(d) *Sicradiscus hirasei* KUZ Z3942. (e)–(h) *Sicradiscus ishizakii* KUZ Z3943, Z3944. (i)–(l) *Sicradiscus pallgergelyi* sp. nov. KUZ Z3950, Z3952. Scale bars: (a), (d), (e), (h), (i), (l) 1000 μm ; (b), (c), (d), (f), (g), (j), (k) 500 μm



879

880 FIGURE 5 Parietal and palatal plication of *Sicradiscus* species. (a), (c), (e), (g), (i), (k), (m),
 881 (o), (q), (s), (t), (u), (w), (y), (aa), (ac), (ae), (ag), (ai), (ak), (am), (ao), (aq), (as), (au), Parietal
 882 lamellae. (b), (d), (f), (h), (j), (l), (n), (p), (r), (t), (v), (x), (z), (ab), (ad), (af), (ah), (aj), (al),

883 (an), (ap), (ar), (at), (av), Palatal plicae. (a)–(p), *Sicradiscus hirasei*, KUZ Z3942. (q)–(af),
884 *Sicradiscus ishizakii*, KUZ Z3943–Z3944. (ag)–(av), *Sicradiscus pallgergelyi* sp. nov., KUZ
885 Z3950, Z3952. Aperture direction is indicated under (a) and (b). Gray drawings represent
886 vestigial parts of lamellae
887

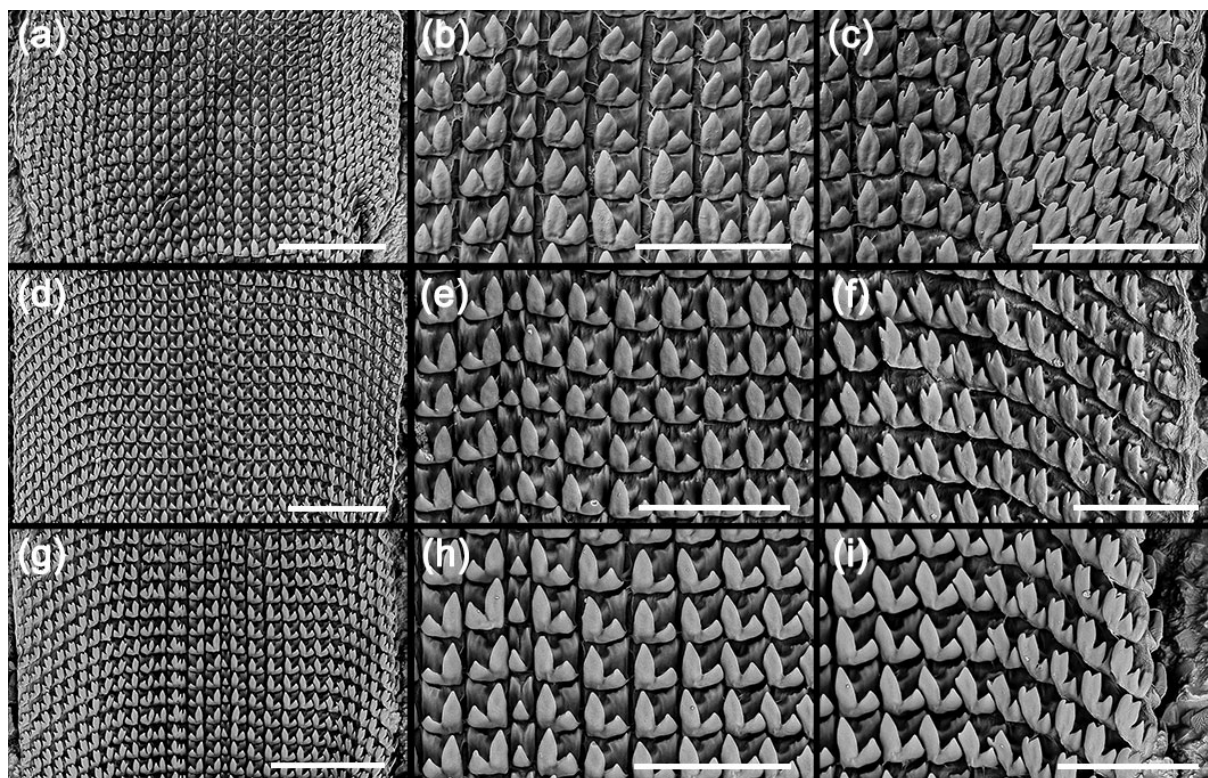


FIGURE 6 Radulae of *Sicradiscus* species. (a), (d), (g) Middle parts of radulae. (b), (e), (h) Central and lateral teeth. (c), (f), (i) Lateral teeth. (a)–(c) *Sicradiscus hirasei* KUZ Z3942. (d)–(f) *Sicradiscus ishizakii* KUZ Z3943. (g)–(i) *Sicradiscus pallgergelyi* sp. nov. KUZ Z3952. Scale bars: (a), (d), (g) 100 µm; (b), (c), (e), (f), (h), (i) 50 µm

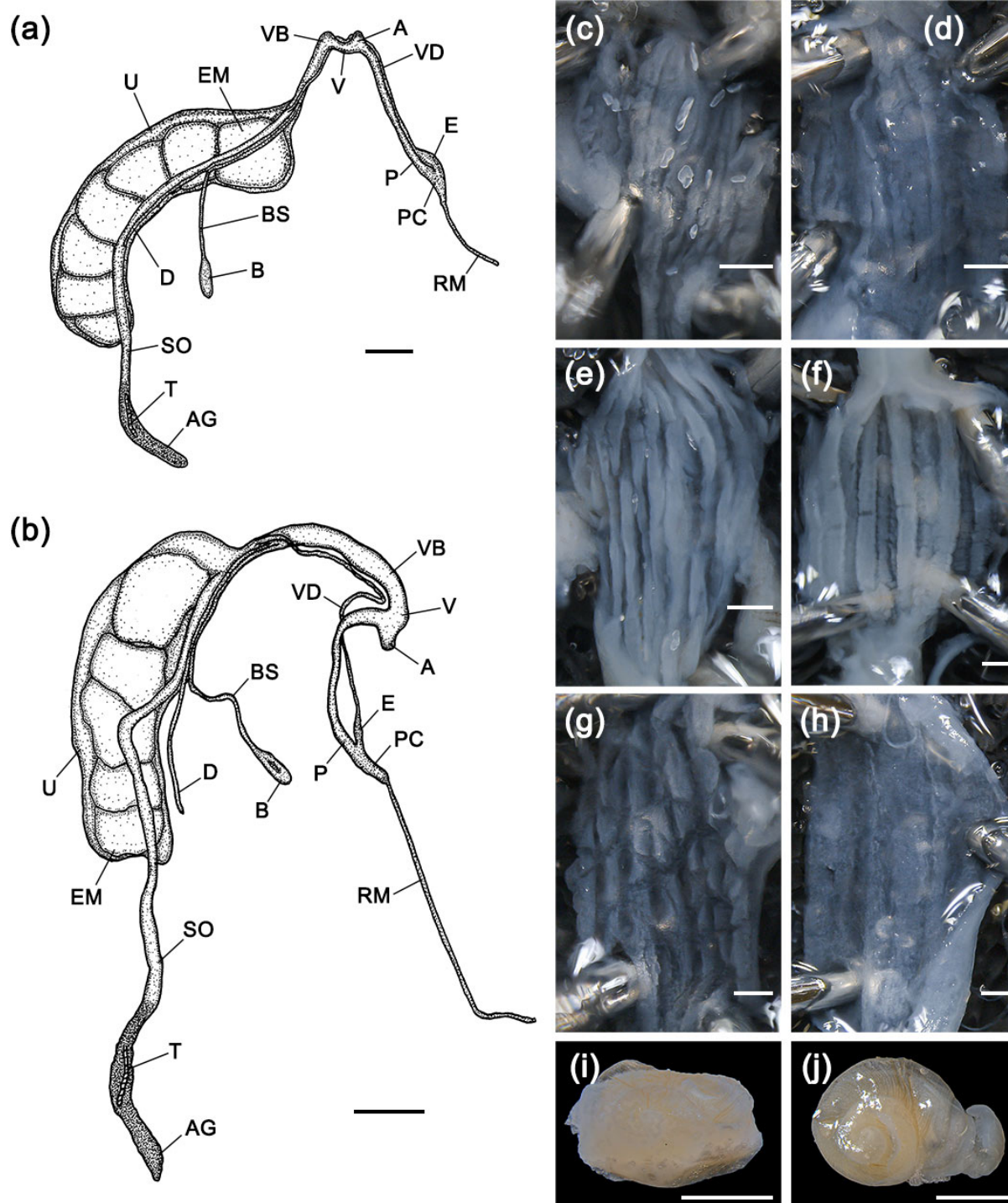


FIGURE 7 Reproductive anatomy of *Sicradiscus* species. (a), (b) Reproductive system. (c), (e), (g) Inner penial wall. (d), (f), (f) Inner vaginal wall. (i), (j) Embryo. (a), (e), (f), (i) *Sicradiscus ishizakii*, KUZ Z3943. (b), (g), (h), (j) *Sicradiscus pallgergelyi* sp. nov., KUZ Z3949 (c), (d) *Sicradiscus hirasei*, KUZ Z3942. Atriums are on the upper side of the images of (c)–(h). Abbreviations: A, atrium; AG, albumen gland; B, bursa of the bursa copulatrix; BS, stalk of bursa copulatrix; D, diverticulum; E, epiphallus; EM, embryo; P, penis; PC, penial caecum; RM, retractor muscle; SO, spermoviduct; T, talon; U, uterus; V, vagina; VB, vaginal bulb; VD, vas deferens. Scale bars: (a), (b), (i), (j) 1000 μ m; (c)–(h) 200 μ m

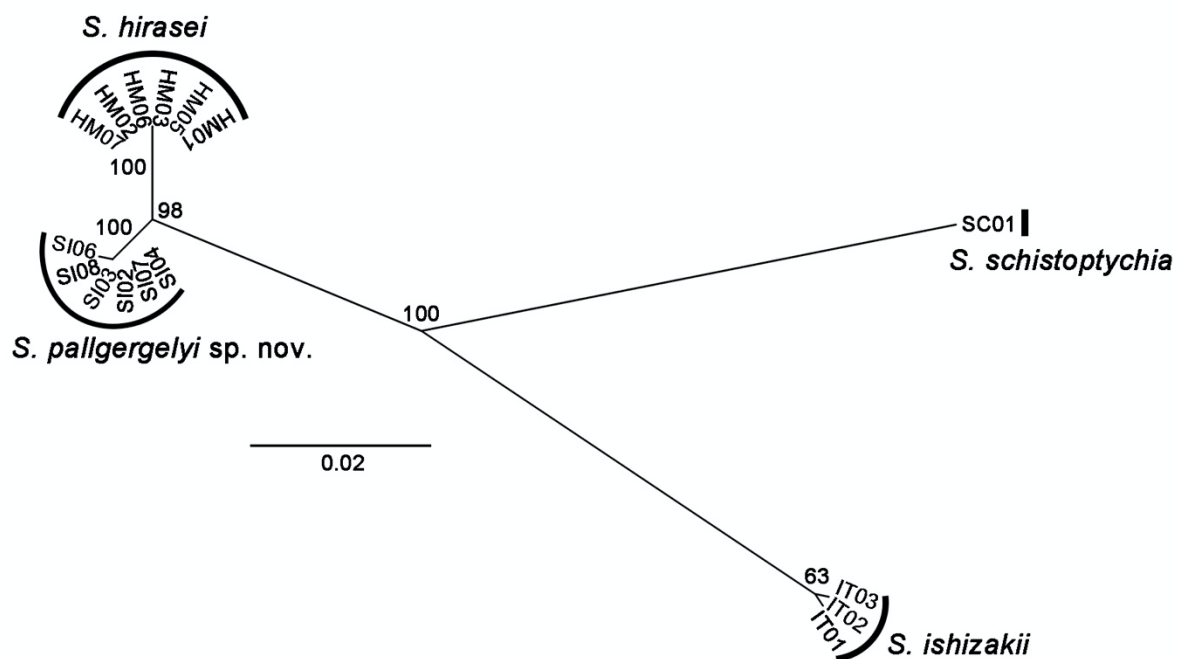


FIGURE 8 Maximum likelihood tree built from COI DNA barcodes of three insular *Sicradiscus* species and *S. schistoptychia* (the type species of *Sicradiscus*). Numbers on nodes represent bootstrap values

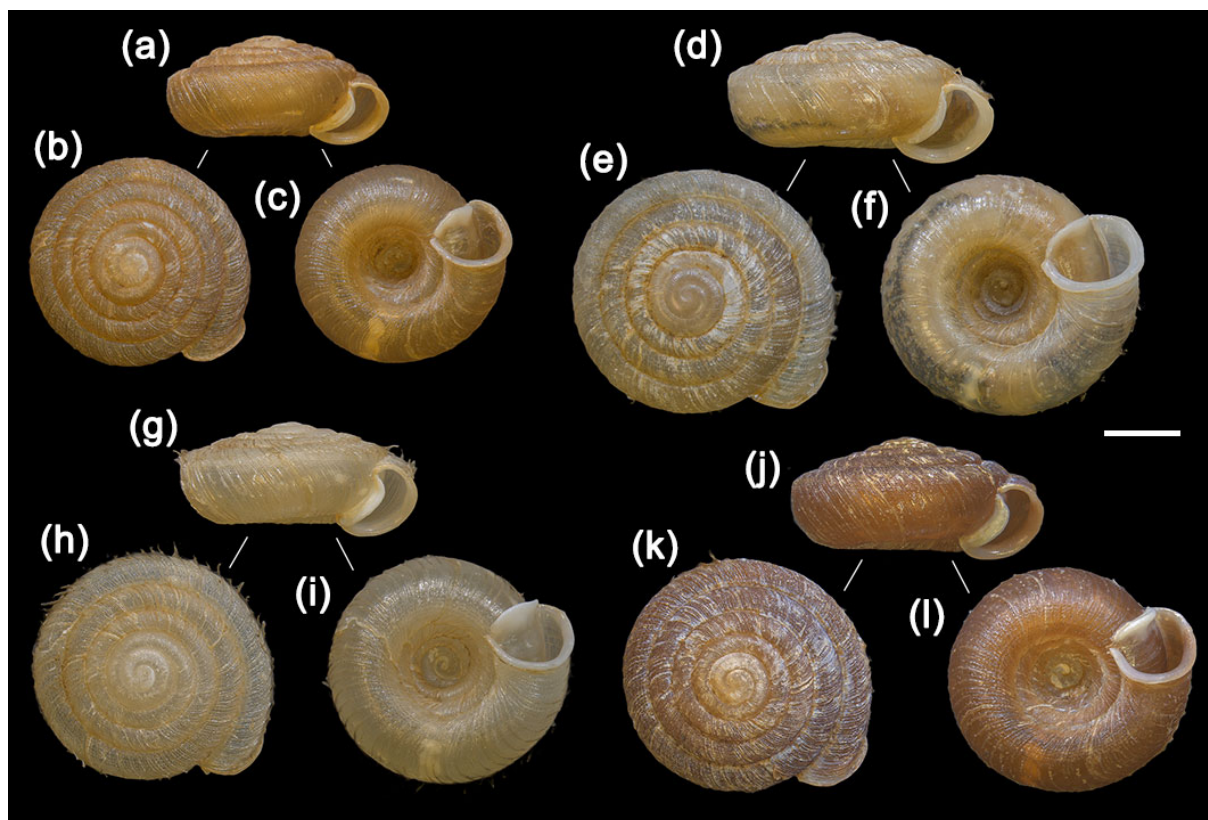


FIGURE 9 Adult shells of *Sicradiscus* species. (a)–(c) *Sicradiscus hirasei* KUZ Z3942. (d)–(f) *Sicradiscus ishizakii* KUZ Z3943. (g)–(l) *Sicradiscus pallgergelyi* sp. nov. (g)–(i) Holotype, KUZ Z3947. (j)–(l) Paratype, KUZ Z3949. Scale bar: 2 mm



914

915 FIGURE 10 Living specimen of *Sicradiscus pallgergelyi* sp. nov. Scale bar: 1 mm